Final Report

Cover Page

Report Number:	DOE-PBL-20768
DOE Award Number:	DE-SC0020768
Sponsoring Program Office:	DOE Office of Science
Name and Address of Recipient:	Particle Beam Lasers, Inc. 18925 Dearborn Street Northridge, CA 91324-2807
Project Title:	Overpass/Underpass coil design for high field dipoles
Principal Investigator:	Ramesh Gupta
Team Members BNL:	Ramesh Gupta, Michael Anerella, Paul Kovach, Jesse Schmalzle,
Team Members PBL:	Stephen Kahn, Robert J. Weggel, Ronald Scanlan, Erich Willen, James Kolonko, Delbert Larson, Albert Zeller

Acknowledgement: This material is based upon work supported by the U.S. Department of Energy, Office of Science, Office of Basic Energy Sciences, under Award Number DE-SC0020768.

Project Summary / Abstract

Company Name and Address: Particle Beam Lasers, Inc.
18925 Dearborn Street
Northridge, CA 91324-2807

Principal Investigator: Ramesh Gupta

Project Title: Overpass/Underpass coil design for high field dipoles

Purpose of Research, Research Carried Out, and Research Findings:

This Phase I has laid the groundwork for a "Proof-of-Principle" demonstration of an ~11 T Nb_3Sn dipole based on the novel overpass/underpass (also called cloverleaf) end design for high field dipole magnets of block-coil geometry. Block coil dipoles are appealing for their simplicity in the body of a magnet, but less so in the ends of the blocks that must dodge the beam tube. The required bending of the conductor typically is in the hard direction of the broad cable, and therefore must be very gradual, to avoid conductor degradation from excessive strain; the end regions become undesirably long.

The overpass/underpass or cloverleaf end geometry is designed to overcome the above-mentioned shortcomings. The conductor clears the bore tube at the ends by replacing the hard-way bends by a gentle twist in a 270° ramped turn. The end regions extend relatively little beyond the straight legs. The strain on the cable in the ends remains low if the conductor is allowed to tilt to minimize its strain.

A proof-of-principle demonstration of this design is to be carried out in Phase II for the pole coils in a 2-in-1 common-coil dipole. These pole coils are required to obtain good field quality, and must deviate from simple flat racetracks whenever necessary to clear the bore tube. Such a demonstration, which so far has never been done before, is possible within the budget of a Phase II SBIR, thanks to the design of BNL's dipole DCC017. The dipole has a large, easily accessible midplane gap in which insert coils can be tested as an integral part of the magnet without need for any disassembly and reassembly.

The Phase II proposal leverages Phase I's great progress in the magnetic, mechanical, and engineering designs of the overpass/underpass geometry. Phase I also wound a practice coil of unreacted Nb_3Sn Rutherford cable and inserted it inside DCC017 as a mockup assembly.

The Phase II work plan includes further magnetic and mechanical design of this proof-of-principle dipole, which will be tested to reach ~11 T. Once the design has been successfully demonstrated, the overpass/underpass end geometry likely will be used in block coil designs in addition to the common coil. For example, the present 20 T HTS block coil design at CERN is based on the overpass/underpass (or cloverleaf) design. We will also perform the preliminary design of a 16 T dipole based on Nb_3Sn and a 20 T hybrid dipole design based on both Nb_3Sn and High Temperature Superconductors (HTS). We will examine how to carry out industrial production and commercialization of the magnets based on the overpass/underpass design.

Potential Applications of the Research:

Block coil dipoles with end windings based on the overpass/underpass design are appealing for a variety of accelerator applications, and for other scientific research needs. The overpass/underpass design, if successfully demonstrated, will reduce both the stored energy and length of the magnet and may improve performance in machines such as the Future Circular Collider (FCC), which in itself offers a market of several billion dollars.

Table of Contents

1.0 Introduction

The goal of this proposal is to develop an innovative overpass/underpass coil design for high field block coil dipoles. This report summarizes the work performed during Phase I on the magnetic, mechanical, and preliminary engineering design of the overpass/underpass (or cloverleaf) geometry, as well as the winding of a practice coil to demonstrate a ~11 T proof-of-principle dipole in Phase II. This work is performed under the Small Business Technology Transfer (STTR) Phase I grant (DE-SC00020768) to Particle Beam Lasers, Inc. (PBL) and Brookhaven National Laboratory (BNL) to develop a novel end geometry for block coil dipoles as an alternative to the conventional design of lifted ends, which tend to be longer and prone to put excessive strain on the brittle Nb_3Sn conductor.

The High Energy Physics Advisory Panel (HEPAP) subpanel on Accelerator R&D has recommended to "Aggressively pursue the development of Nb_3Sn magnets suitable for use in a very high-energy proton-proton collider" [1]. The 2014 Particle Physics Project Prioritization Panel (P5) recommended that the United States Department of Energy (DOE) research efforts should "Participate in global conceptual design studies and critical path R&D for future very high-energy proton-proton colliders and continue to play a leadership role in superconducting magnet technology focused on the dual goals of increasing performance and decreasing costs".

Our Phase I work, the basis for a strong Phase II proposal, has included engineering design work well beyond that promised in the Phase I proposal. The overpass/underpass design, upon successful demonstration, will be applicable for any block coil dipole (either single aperture or dual aperture common coil) made of NbTi, Nb_3Sn and/or High Temperature Superconductors (HTS) for high energy accelerators, such as the proposed Future Circular Collider (FCC).

2.0 Technical Approach

This proposal is to develop an innovative overpass/underpass coil design [2, 3] for the ends of high field block coil dipoles of Nb_3Sn Rutherford cable [4-7]. The block coil dipole design is an alternative to conventional cosine theta dipoles, with a goal of increasing performance and/or reducing costs. Block coil geometries have the virtue of simplicity of the cross-section. Several magnets based on various block coil designs have been designed, built, and tested. These include (a) single-aperture, or conventional 2-in-1 block coil designs with two independent coils and (b) 2-in-1 common coil [8] designs, in which the same coil is shared between the two apertures. In both designs, to clear the bore tube, the ends of several blocks must depart from the simplicity of the flat racetrack coil design. The cable in the ends of those blocks needs to be splayed--lifted in the hard direction (edgewise)--and/or have a reverse bend, as in dog-bone ends, which is difficult to support during the coil winding and during assembly. Also, it is difficult to maintain winding tension or apply pre-stress without damaging the conductor. The complications in the end geometry may contribute to degraded performance of block coil magnets, particularly those built with Nb_3Sn, which is brittle. The overpass/underpass design addresses this issue for high field magnet coils. Another major disadvantage of conventional block coil magnets has been that their ends are much longer than those of conventional cosine theta designs. The overpass/underpass design (also called the cloverleaf end design) overcomes that disadvantage.

2.1 Conventional Block Coil Designs with Lifted Ends

Photos of an early block coil design by Sampson at BNL are given in Fig. 2.1, with the coil cross-section shown on the left, and the magnet ends, with Rutherford cable gently lifted, shown on the right [4].

Figure 2.1: Nb_3Sn block coil dipole with cross-section (left) and lifted ends (right).

Since then, several more Nb_3Sn block coil designs with lifted ends have been designed, and a few built: (a) a 13.8 T, 36 mm aperture dipole (named HD2) at Lawrence Berkeley National Laboratory (LBNL) [5], (b) a 13 T, 100 mm aperture dipole (FRESCA2) at CERN [6], and (c) a high field block coil magnet at Texas A&M [7]. The ends of these magnets are shown in Fig. 2.2, showing how the cable is lifted to clear the bore tube.

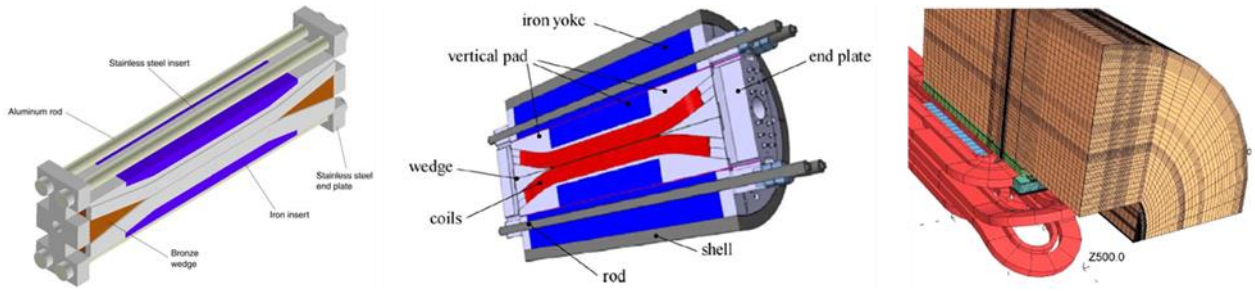

Figure 2.2: Models of block coil dipoles with lifted ends to clear the bore tube: (a) HD2 at LBNL on the left, (b) FRESCA2 dipole at CERN in the middle, and (c) Block coil dipole at Texas A&M on the right.

<u>Issues with Lifted Hard-way Bends in Block Coil Dipoles</u>

All block coil dipole designs presented above require the cable to be bent the *hard*-way (edgewise) on each side of the mid-plane to clear the bore tube at the ends (see Fig. 2.2). Although most Nb_3Sn coils are fabricated using the react-after-winding ("*wind and react*") approach, a hard-way bend of the unreacted cable can cause strands to become dislocated and thus sensitive to damage when the coils are handled and after the reaction heat treatment. In addition, it is difficult to provide adequate support of the turns in this hard-way bend transition area, and this may contribute to excessive magnet training. To avoid *excessive strain*, the ends are typically much longer in block coil designs than those in their counterpart cosine theta designs. This increase in end length decreases the overall field integral of the magnet for a given length, which is undesirable.

Issues with the Ends of Pole Blocks of Common Coil Dipoles

Some of the issues that are of concern in the several single-aperture block coil cross-sections are also of concern in most designs of the pole blocks of a 2-in-1 common coil dipole [8].

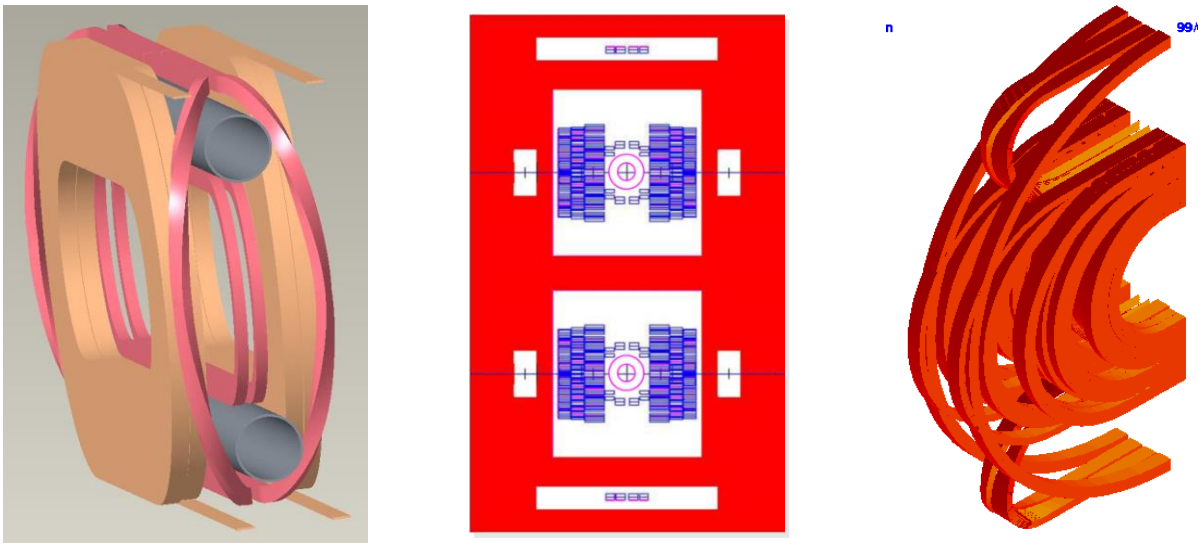

Figure 2.3: Common coil design with the turns of pole blocks lifted sideways to clear the bore tube (left), common coil cross-section that allows all coils to be simple racetrack coils (middle), but that requires some turns to return away from the aperture, thus subtracting from, rather than contributing to, the field in the bore.

Although the majority of turns in the common coil geometry have simple racetrack coil ends (referred to as the main coils, as shown by the golden-brown color in Fig. 2.3, left), some need to be lifted sideways to clear the bore tube (referred to as the pole coils – shown by the pink color in Fig. 2.3, left). Another design option is to have turns of some pole blocks return away from the aperture as shown in Fig. 2.3 (center) for the cross-section and Fig. 2.3 (right) for the ends. This keeps the design simple; however, it is at the expense of wasteful use of the conductor and an increase in yoke size to accommodate the turns on the return side. As explained later, the proposed overpass/underpass design also offers a design option for pole blocks to clear the beam tube in the common coil design.

2.2 Novel Overpass/Underpass (Cloverleaf) Design

To overcome excessive strain and associated concerns on magnet performance, an alternative end geometry, called the overpass/underpass (or cloverleaf) has been proposed [2, 3]. The overpass/underpass design, as explained below, replaces the *hard-way* bend by a *gentle twist.* This greatly reduces the strain on the cable. Another major benefit of this design, as discussed more in the next section, is a major reduction in the length of the ends of the block coil designs.

In an example considered here, the total strain in the ends of the overpass/underpass design (a combination of strain from the twisting and from the bending) is smaller by approximately a factor of five despite a five-fold reduction in the length of the overpass/underpass ends as compared to that of the conventionally lifted ends. This estimate is made for a cable having a width of 15 mm and thickness of 2.0 mm and the length/radius of the overpass/underpass ends being 50 mm compared to 250 mm for conventional lifted ends. A more detailed and complete modelling of these strains will be carried out as a part of the Phase II proposal. The OP/UP approach may also

allow Nb_3Sn magnets to be fabricated using a wind-after-reacting approach since the strains are much reduced.

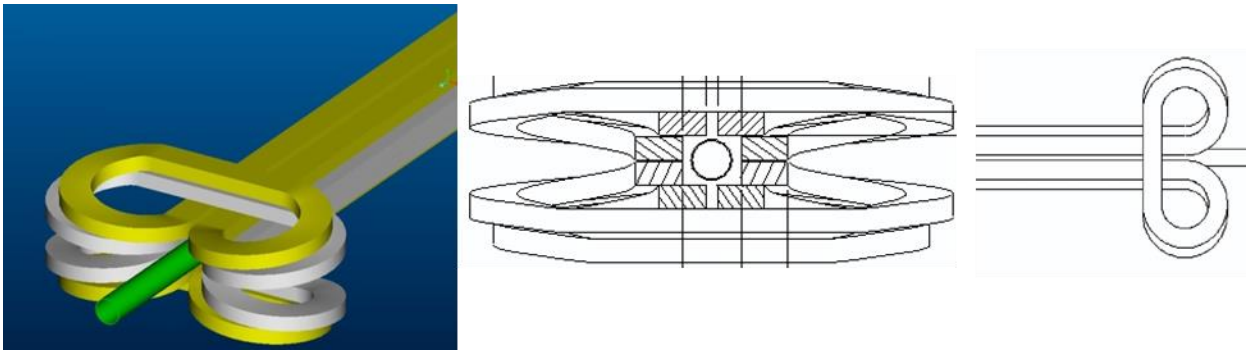

Figure 2.4: Overpass/Underpass design concept [7] for clearing the bore tube (left) in racetrack coil dipoles. A view from the side (middle) and top (right) showing the cross-section and coils (including ends) of the overpass/underpass design.

Fig. 2.4 illustrates the concept [2] of a block-coil dipole based on the overpass/underpass design for the magnet ends. An easy way to understand this concept (the path of the cable) is to imagine the cable as tracing the path of an automobile reversing direction via an overpass/underpass bridge (see Fig. 2.4, right). The cable (or automobile) clears the beam (traffic) via the overpass/underpass, returning to its original highway with reversed direction of travel, as desired. The coil ends clear the beam tube without a hard-way bend. Moreover, unlike in dog-bone ends [4], no reverse curvature is involved. The cable traverse involves a twist or tilt, as typical on an overpass/underpass of a high-speed expressway. This twist is much gentler than in a "Twisted Stacked-Tape Cable [9]" made with HTS tape and should not degrade the Nb_3Sn.

For winding the coil, the turns are wound outside-in (i.e., the turn furthest away from the center is wound first), with successive turns layering naturally. The cable clears the bore tube as it first traverses away from the aperture and moves up or down over the mid-plane the same way the cable does in layer wound solenoidal coils. The bend radius can be chosen independently of the bore radius (perhaps limited by other constraints such as the size of the coldmass) to obtain the desired reduction in the strain. The cable will tend to have a constant perimeter end (i.e. the total length of the tape is invariant across the width of the tape).

The primary purpose of the STTR project is to develop and demonstrate the overpass/underpass design for a high field Nb_3Sn racetrack coil block made with Rutherford cable. Two designs of interest are: (a) coils at or near the mid-plane of the single-aperture block coil dipoles and (b) pole blocks of the 2-in-1 common-coil dipoles. In both cases conductors in the ends of some coil blocks need to be lifted-up to clear the bore. The proposed design will not only avoid severe bends in the hard direction but will also eliminate reverse bends and make the ends much shorter.

Shorter Ends of Overpass/Underpass Coils

A major disadvantage of lifted ends in block coil designs is that they are excessively long, in order to keep the strain low when the cable is bent in the hard direction. Fig. 2.5 compares the length of the coil (for the same length of the magnet straight section) when overpass/underpass ends are used (see the lower coil in Fig. 2.5) instead of lifted ends (the upper coil in Fig. 2.5).

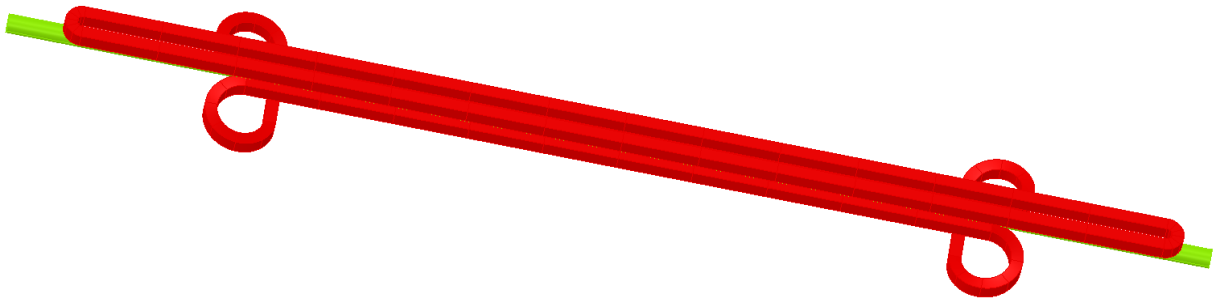

Figure 2.5: A comparison of the length of the ends in a coil with overpass/underpass ends (the lower coil) and a coil with lifted ends (the upper coil) needed to clear the bore tube (green).

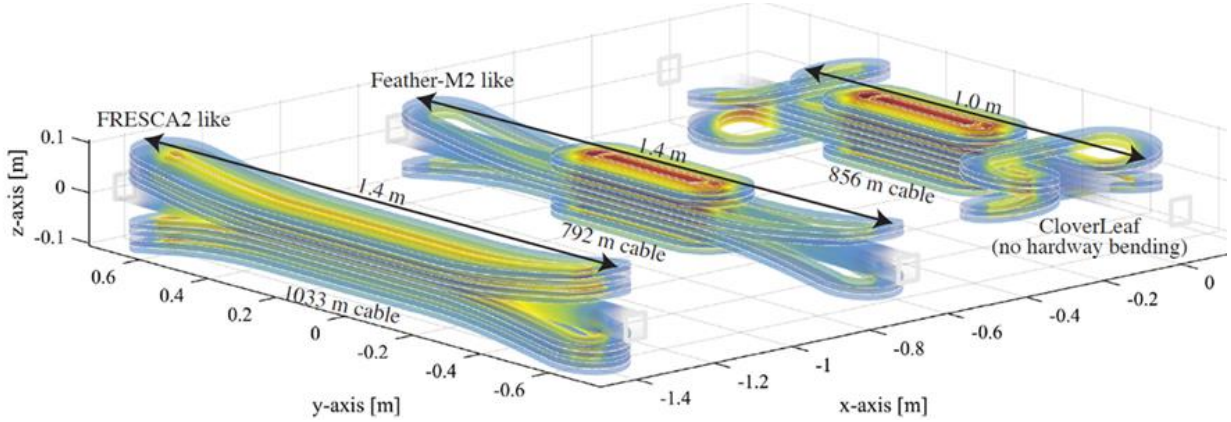

Figure 2.6: Comparisons of the length of the ends in coils with lifted ends (left & center) and a coil made with overpass/underpass ends (right) needed to clear the bore tube [10].

This virtue was also noted by J. van Nugteren, et al., and presented by CERN group in several publications [10-13]. Regular updates on this program are available at the "researchgate site", see "Project log" https://www.researchgate.net/project/Dipole-HTS-Magnets-at-CERN [14]. An illustration from the EUCAS paper [10] is shown in Fig. 2.6. In the FRESCA2 design, the length was about 400 mm for each end (the end-to-end coil length is about 1400 mm, but the straight section is only about 700 mm).

Two coils based on the overpass/underpass geometry were built with pre-reacted HTS tapes a few years ago as a part of an SBIR with Energy to Power Solutions (e2P) as the principal contractor collaborating with Brookhaven National Laboratory (BNL) as a subcontractor. The HTS coils were tested only at 77 K. Those test results, as partially presented at the 2016 Low Temperature Superconductor Workshop (LTSW16), showed no measurable degradation in the overpass/underpass geometry [15].

Despite the advantages mentioned above, the end geometry itself is more complicated for winding the coils than that in a simple racetrack coil and will require a more complicated support structure. Furthermore, the strain, though expected to be lower than that in a lifted end-design and in other designs, will require careful calculation. This report summarizes the work performed during Phase I to address these issues. Initial 2-D and 3-D magnetic and mechanical analyses of the design have been performed, along with the preliminary engineering design, winding of the practice coil.

2.3 Summary of the Phase II Proposal

The key goal of the Phase II proposal is the construction and test of the novel overpass/underpass (or cloverleaf) geometry in a proof-of-principle demonstration with Nb_3Sn Rutherford cable at a field of ~11 T. Such a demonstration is possible within the budget of a Phase II, thanks to the unique capabilities of BNL's dipole DCC017 [16-18]. It has a large, easily accessible open space in which new coils can be inserted and tested as an integral part of the magnet without any need for disassembly and reassembly [18]. The Phase II proposal is built upon the progress and experience of work performed in Phase I (described in the following sections in detail), where we carried out the magnetic, mechanical, and preliminary engineering design of the overpass/underpass geometry and how the coil will be wound, reacted, impregnated, and assembled in a structure that will be assembled with the common coil dipole for the proposed proof-of-principle 11 T test. The ends of the coil will be located beyond the central field of the magnet (as expected in any overpass/underpass design) to reduce the magnetic forces in the end regions. The transverse ends between the "cloverleafs" of the coil were designed with a convex curve, as CERN employed [14], to facilitate conductor contact with the winding surface in these regions. We also chose, located, and secured the Nb_3Sn cable that will be used in the Phase II coil. This is a left-over Nb_3Sn cable such as used in previous magnets with good results.

The width of each OP/UP coil (including ends) must be at least two cable-widths plus a small gap between the body and cloverleaf section at the crossover. While DCC017 offers an opportunity to demonstrate a proof-of-principle overpass/underpass high field dipole, it also restricts and complicates the design. For example, to install the OP/UP coil without disassembling the magnet DCC017, we need an opening of at least two cable widths to insert one coil. To insert a two-coil package, the opening must be at least either (a) four cable widths, if the two coils have the same length, or (b) at least three cable widths, if the two coils are of different lengths, with staggered placement of the ends. Such restrictions and complications would not be present in a new magnet. We studied the latter option in detail (see section 6 on preliminary engineering design) but settled for a one-coil test to fit the Phase II budget.

Phase I work included two practice windings, first a single turn coil with the geometry of the Phase I proposal, and then a 5-turn practice coil with the evolved convex curve in the end region as mentioned above. The second coil was wound with the same geometry and the same number of turns and using the similar unreacted Nb_3Sn Rutherford cable that will be used in Phase II.

3.0 Selection of the Conductor for Phase II

Selection of the superconducting cable for Phase II received considerable attention. The cable width must be narrow enough to fit inside the dipole DCC017, and its critical current must be high enough to run in series with the main coil. Moreover, it should be available soon, to fit the schedule of the SBIR/STTR program. Fortunately, the Nb_3Sn Rutherford cable developed for the LARP Long Racetrack Series (LRS) magnet program [19] satisfies all these requirements. The LARP LRS001 magnet reached a nominal "plateau" at 9596 A, at a peak field in the coils of 11 T. This is what we desire based on our calculations. Several left-over pieces of this cable have been secured, and each is long enough to satisfy the above requirements.

The cable for the LRS magnets used the Rod-Restack Process (RRP) wire from Oxford-Instruments Superconducting Technology (OI-ST). The strand diameter was nominally 0.7mm with the 54/61 design. The average Cu/non-Cu ratio of the strands was 0.87, and when reacted at 650C/48 hours it has a RRR greater than 200. Low field stability measurements show that strands reacted with an optimized heat treatment had a minimum critical current I_c (12T, 4.2K) of 560 A. We will follow the same heat treatment that was optimized for the LARP cable.

The rectangular cable was fabricated with 20 strands. After cabling, the cable was annealed for 8 hours at 200C and subsequently re-rolled to the following dimensions, width: 7.793 ± 0.050 mm, mid-thickness: 1.276 ± 0.010 mm.

The properties of the strands are shown in Table I, and of the cable, in Table II.

TABLE I
STRAND PROPERTIES MEASURED BY OST

Billet Number	8647	8648
Strand Diameter, mm	0.7	0.7
No. of subelements	54	54
Cu fraction	46.1 ±0.2%	46.3 ±0.2%
I_c (12 T, 4.2K), A (1)	562 ± 10	560 ± 18
J_c (12 T, 4.2K) , A/mm^2	2752 ± 42	2711 ± 96
RRR	195 ± 10	212 ± 29

(1) reaction cycle 210º C /48h + 400º C /48h + 665º C /48h

TABLE II
PROPERTIES OF CABLE

Cable ID	942R	949R
Number of Strands	20	20
Pre-anneal sizes, mm	7.855 x 1.306	7.848 x 1.307
Re-roll sizes, mm	7.828 x 1.277	7.828 x 1.274
Cable Pitch, mm	54.5	55.0

4.0 Magnetic Design Analysis

Extensive magnetic analyses were performed to evaluate several designs and their variations. This included (a) a dipole DCC017 completely rebuilt, integrating its Nb_3Sn coils with new overpass/underpass coils, (b) a dipole in which new overpass/underpass coils are inserted and integrated with DCC017 without taking the DCC017 apart, (c) several variations of (b) with a range of overpass/underpass coil numbers and geometries, and (d) other magnet designs in which all coils are built new. Assembling new overpass/underpass coil(s) and integrating them with DCC017 without disassembly provides the least expensive proof-of-principle magnet but also will also be the most complicated, as it involves several restrictions in the geometry. It allows the novel overpass/underpass to be fully tested in the budget of Phase II and provides the testing of the design at high fields.

The following subsection summarizes key select cases.

4.1 DCC017 Rebuilt with Overpass/Underpass Coils

A field quality rebuild of the common coil dipole DCC017 will require pole coils in addition to the main coils [20] which have simple racetrack coil geometry. These pole coils can be operated in series with the main coils. Even though such a DCC017 was not designed with the field quality considerations, it has been shown that the additional pole coils can bring all harmonics within a few units. The calculated multipoles in the as-built 31 mm bore dipole DCC017 and in one of the optimized designs of the pole coils are given in Table III at a reference radius of 10 mm.

TABLE III. LEFT SIDE SHOWS THE CALCULATED MULTIPOLES IN AS-BUILT DCC017, SHOWING LARGE VALUES FOR b_3 AND a_2. RIGHT SIDE SHOWS THE CALCULATED MULTIPOLES WITH FULLY OPTIMIZED POLE COILS ADDED, SHOWING ALL VALUES BELOW A FEW UNITS.

DCC017 without pole coils (present design)

```
MAIN FIELD (T) ....................................     0.995409
MAGNET STRENGTH (T/(m^(n-1)) ......................       0.9954

NORMAL RELATIVE MULTIPOLES (1.D-4):
b 1:  10000.00000  b 2:      0.00000  b 3:    187.58719
b 4:     -0.00000  b 5:     -2.01358  b 6:      0.00000
b 7:     -0.13995  b 8:     -0.00000  b 9:      0.00365
b10:      0.00000  b11:      0.00136  b12:     -0.00000
b13:     -0.00014  b14:      0.00000  b15:     -0.00000
b16:     -0.00000  b17:      0.00000  b18:      0.00000
b19:     -0.00000  b20:     -0.00000  b

SKEW RELATIVE MULTIPOLES (1.D-4):
a 1:     -0.00000  a 2:   -192.09501  a 3:      0.00000
a 4:      6.49804  a 5:     -0.00000  a 6:      0.33413
a 7:      0.00000  a 8:     -0.03499  a 9:     -0.00000
a10:     -0.00209  a11:      0.00000  a12:      0.00053
a13:     -0.00000  a14:     -0.00002  a15:      0.00000
a16:     -0.00000  a17:     -0.00000  a18:      0.00000
```

DCC017 with additional pole coils optimized for field quality

```
MAIN FIELD (T) ....................................     1.065489
MAGNET STRENGTH (T/(m^(n-1)) ......................       1.0655

NORMAL RELATIVE MULTIPOLES (1.D-4):
b 1:  10000.00000  b 2:     -0.00000  b 3:      0.00071
b 4:     -0.00000  b 5:      0.00045  b 6:     -0.00000
b 7:      2.69589  b 8:     -0.00000  b 9:      0.38260
b10:     -0.00000  b11:     -0.06197  b12:      0.00000
b13:     -0.02446  b14:      0.00000  b15:     -0.00522
b16:      0.00000  b17:      0.00080  b18:      0.00000
b19:      0.00096  b20:      0.00000  b

SKEW RELATIVE MULTIPOLES (1.D-4):
a 1:      0.00000  a 2:      0.00049  a 3:      0.00000
a 4:     -0.00002  a 5:      0.00000  a 6:      0.30753
a 7:     -0.00000  a 8:      0.26673  a 9:     -0.00000
a10:     -0.01777  a11:     -0.00000  a12:     -0.01224
a13:     -0.00000  a14:     -0.00849  a15:     -0.00000
a16:      0.00121  a17:     -0.00000  a18:      0.00129
```

One possibility of the new additional pole coils is shown in Figure 4.1 (left) and Figure 4.1 (center). The design contains some pole coils that can be a simple racetrack coil as the ends of them do not interfere with the beam tube and some other coils use an overpass/underpass design to clear the beam tube. Fig. 4.1 (right) shows the magnetic model of DCC017 with these pole coils added. The overpass/underpass design brings the end in the plane of the main racetrack coils. The width of the overpass/underpass coil is at least the two-cable widths as the ends are shifted by one cable width (plus any added space at the cross-over). Moreover, overpass/underpass pole coils need to be longer

than the main coils to compensate for the up/down asymmetry in the ends of the common coil magnets in order to obtain a low skew harmonic integral.

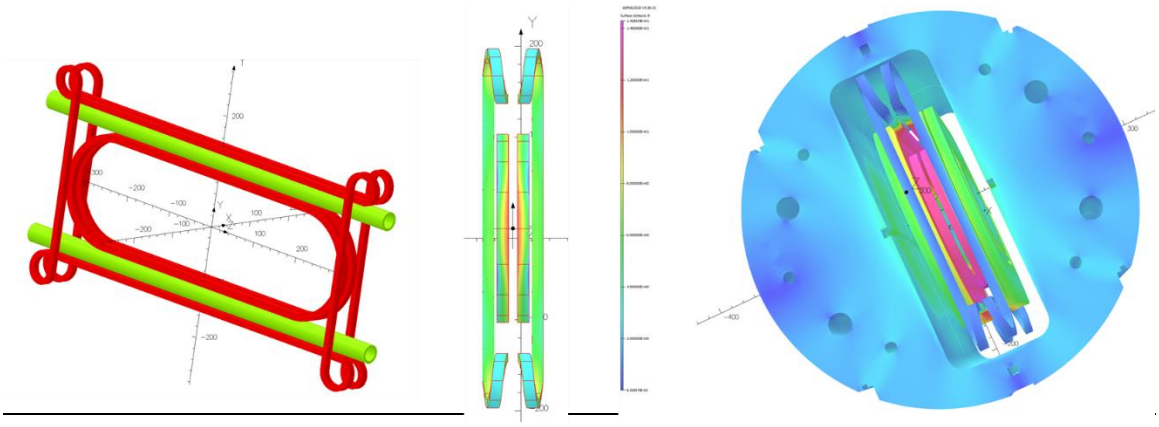

Figure 4.1: Insert pole coils with overpass/underpass coils clearing the bore. Model on the left is a side view and in the middle is a view from the magnet axis. Model on the right shows pole coils inside a possible rebuilt version of the magnet DCC017.

The above design, however, requires the magnet DCC017 to be disassembled and assembled again in a new support structure. The cost of this task is well beyond the budget of Phase II and can be carried out after the lower cost alternate test and assembly proposed in the following three sub-sections.

4.2 Overpass/Underpass Coils in DCC017 with Straight Connect

Fig. 4.2 highlights the difference between a possible rebuilt DCC017 with an overpass/underpass coil (as discussed in the previous section) and the proposed proof-of-principle demonstration where the overpass/underpass coils can be inserted without disassembling the magnet.

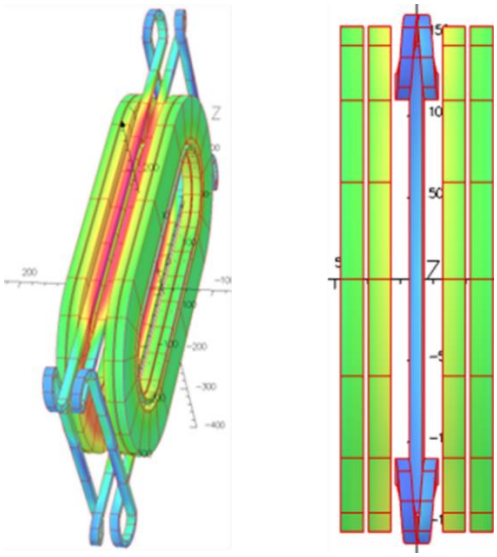

Figure 4.2: Main racetrack Nb_3Sn coils and inserted overpass/underpass Nb_3Sn coils in a rebuilt DCC017 (left) and a proof-of-principle DCC017(right). The overpass/underpass coils are inserted without disassembling the dipole in a lower cost proof-of-principle test.

The horizontal open space inside the magnet DCC017 determines the maximum width of the cable that can be used for making the insert coil. Since the minimum width of each overpass/underpass coil is two cable-widths (as explained earlier), for a pair of coils we would normally need an insulated cable with a width less than ¼ the open space in DCC017, which is ~31 mm. We also need some space for the support structure. Cable that we could locate (see section 3) was a bit wider than desired with insulation. We can still use this cable if one overpass/underpass coil is made longer than the magnet length or the other coil (Fig. 4.3, left). This will not be done in a real magnet but should be acceptable for a proof-of-principle magnet. Even though it makes the design and construction more complicated, it does allow this program to proceed with the cable in hand and which fits all other technical and schedule requirements, as discussed in section 3.

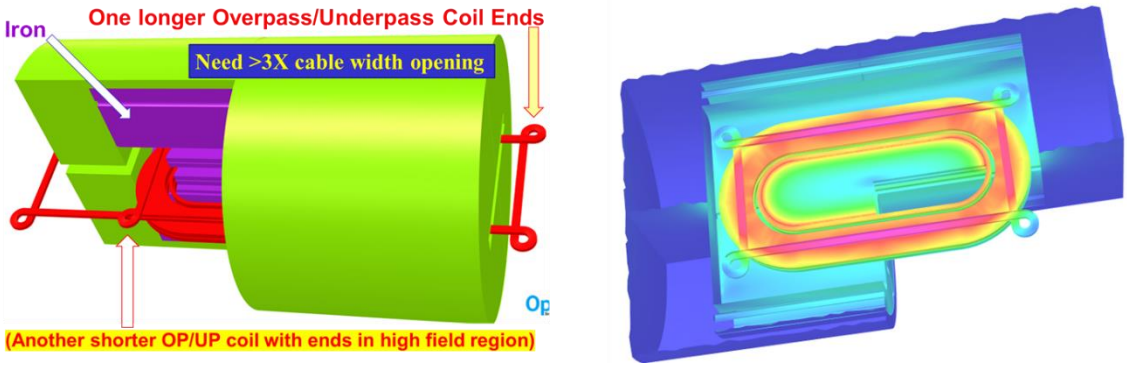

Figure 4.3: OPERA3d model (left) of the two-length coil case allowing a narrower overpass/underpass coil package to be inserted. The yoke iron is shown in purple, stainless-steel (shell and end plates) in green and the coils in red. Two insert overpass/underpass coils of different lengths are sandwiched between the main racetrack coils of the magnet DCC017. The field superimposed on the shorter overpass/underpass insert coil is shown (right). The design is such that the field in the cross-over region is much lower than that in the straight section keeping the stress/strain low in a relatively more complex section of the coil.

Fig. 4.3 (right) shows the cutaway view of the field superimposed over the coil and iron. One can see that the field is lower in the cross-over region with a relatively more complex shape than the straight section of the magnet. This lower field means that the stress/strain on the conductor will be lower as compared to that in the straight section. This provides an extra margin in the coil section where the shape is relatively more complex.

To facilitate the overpass/underpass insert coil test at the highest possible field in the body of the magnet, we chose to place the straight section at the midplane of the magnet (see Fig. 4.4). Moreover, the overpass/underpass coil is oriented such that the coil block in the straight section is closer to the main magnet coil (see Fig. 4.4), which means that the end turns will be closer to the middle of the magnet (see Fig. 4.2, right). The computed maximum field is ~12.5 T at 10 kA when the main coil and the insert coils run in series. Coincidently the quench field in the two is well matched and both the main coil and the insert coil will be closer to their quench performance.

It may be noted that the cable from the upper aperture to lower aperture between the two overpass/underpass sections is connected with a straight section as proposed in our initial design and in the phase I proposal. We will discuss another type of connection in the next section.

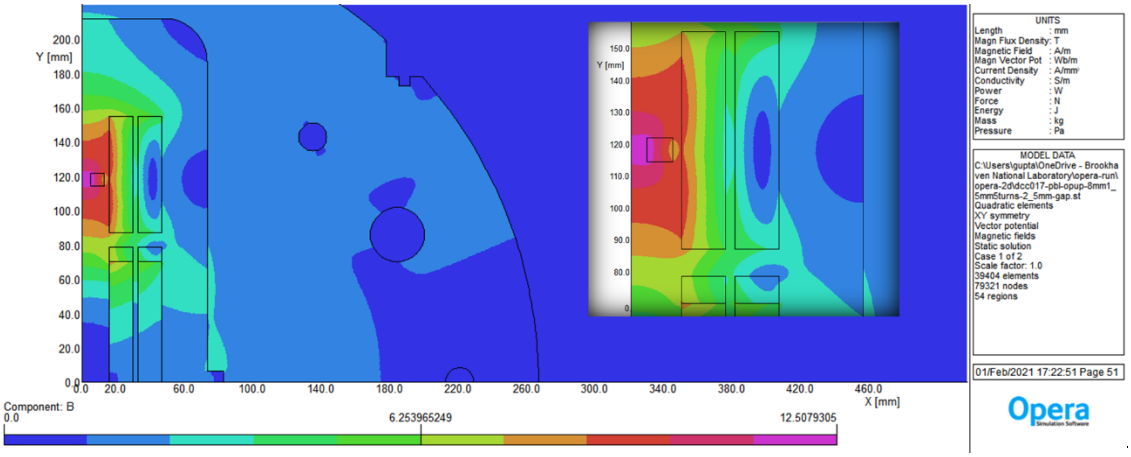

Figure 4.4: Field contours at 10 kA on the straight section of the overpass/underpass coil block at the center of the magnet DCC017 (one symmetric quadrant only). Inset shows the field contour in more detail.

4.3 Overpass/Underpass Coils in DCC017 with Convex Connect

As discussed in section 7, a convex connection is preferred over the straight connection between the two overpass/underpass sections for better winding. A magnetic model is shown in Fig. 4.5 for a five-turn pole with the cable chosen in section 3. To fit two overpass/underpass coils inside DCC017, the length of the two overpass/underpass coils is made different (Fig. 4.5, left) for this proof-of-principle dipole, as mentioned in the previous section. The straight section of the pole coils is closer to the main coils except for some space allowed for a support structure (Fig. 4.5, right), as would be the case in a rebuilt DCC017 or in a new magnet). However, the ends are near the vertical center (Fig. 4.5, right) because of the budgetary restriction in the proof-of-principle magnet and this complication will not be the case in a rebuilt or in a new magnet, as discussed in the previous section. One can see that the field is maximum on the straight section of the insert coil (Fig. 4.5, right).

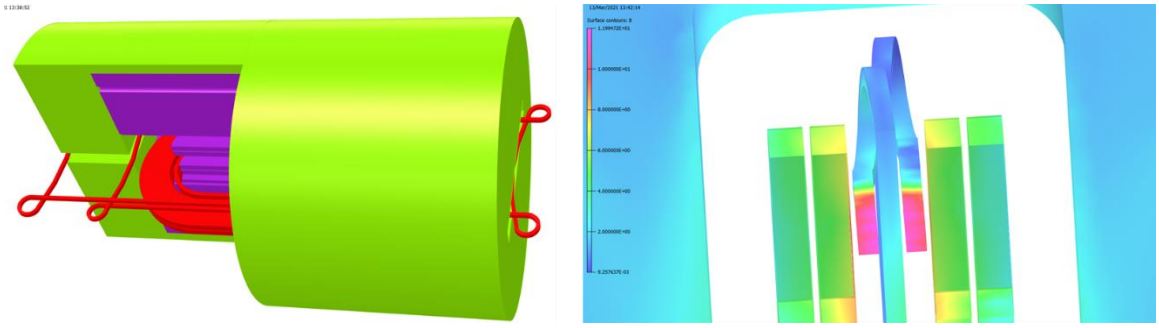

Figure 4.5: OPERA3d model (left) with ¾ model of the yoke in purple, stainless-steel (shell and end plates) in green, and coils in red, including the two overpass/underpass coils with different lengths. Field contours in a cutaway view at 10 kA on the straight section of the overpass/underpass coil block at the center of the magnet DCC017 (one symmetric quadrant only). Inset shows the field contour in more detail.

To visualize the field on the insert coils more clearly, we have shown the cutaway view in Fig. 4.6. Left side of the figure shows the field contours with iron yoke and right side with the yoke hidden. One can see that the field in the crossover or overpass/underpass or cloverleaf section is much smaller than that in the body of the magnet.

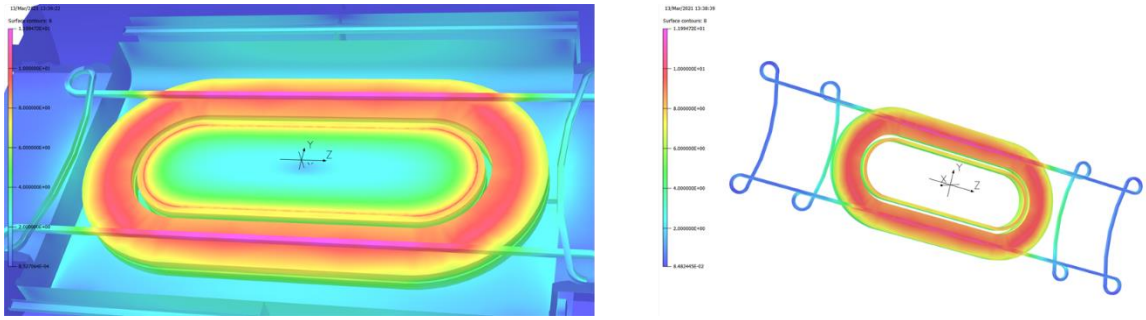

Figure 4.6: A cutaway view to highlight field contours on the coil at 10 kA with a convex connection between the overpass/underpass sections. The model on the left shows the iron whereas the one on the right has the iron hidden. These cutaway views emphasize the field contours on the overpass/underpass insert coil as one can see a lower field region in a relatively more complex section, giving it an extra margin.

4.4 Proof-of-Principle Overpass/Underpass Dipole for Phase II

After performing the detailed magnetic, mechanical, and significant engineering designs, it was found that the two-coil insert can't be accommodated in the Phase II budget. The work for all options was performed in parallel for various levels of detail because of the limited duration of Phase I. The Phase II proposal is to test one overpass/underpass insert coil in the common coil dipole DCC017. The smaller of the two coils is chosen as the ends of it reside in a relatively higher field region and is more representative of the coil in an optimized design of the magnet. As such the one coil test itself will demonstrate all key features of the overpass/underpass design. Fig. 4.7 (with only ¾ of the yoke, stainless steel shell and endplates selected for clarity) shows two different views of the magnet.

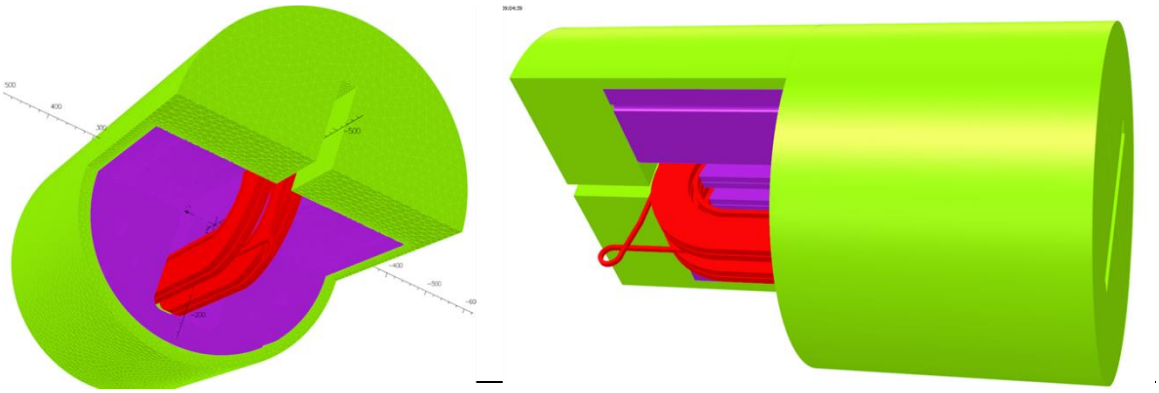

Figure 4.7: OPERA3d model with ¾ of the yoke shown in purple, stainless-steel (shell and end plates) in green, and coils in red. The model shows the main racetrack coils of the magnet DCC017 and one overpass/underpass insert coil in the magnet aperture.

Fig. 4.8 (left) shows the mesh and field contours superimposed on the model and Fig. 4.8 (right) shows the cutaway view field contour superimposed on the coils and iron. One can again see that the field on the insert coil is maximum in the body of the magnet and much less in the overpass/underpass region.

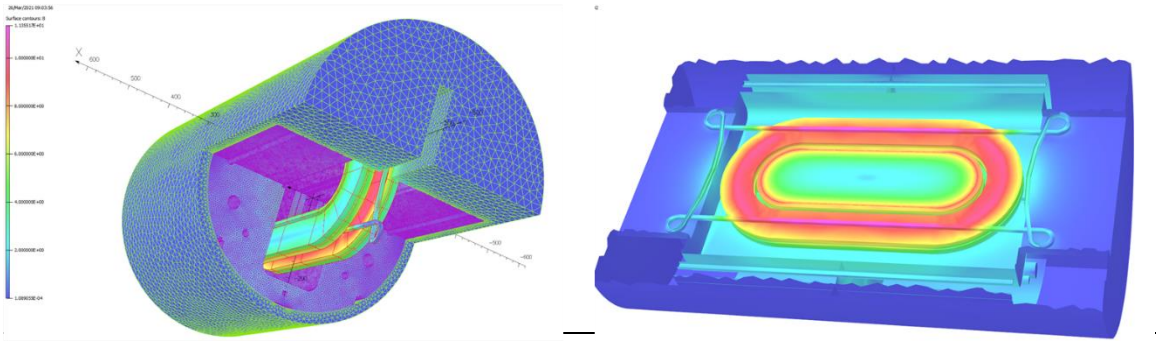

Figure 4.8: Model on the left shows the mesh and field contours superimposed on the yoke and stainless-steel regions and the model on the right shows the cutaway view field contour superimposed on the coils and iron. One can see the highest field (purple) in the straight section region of the insert coil.

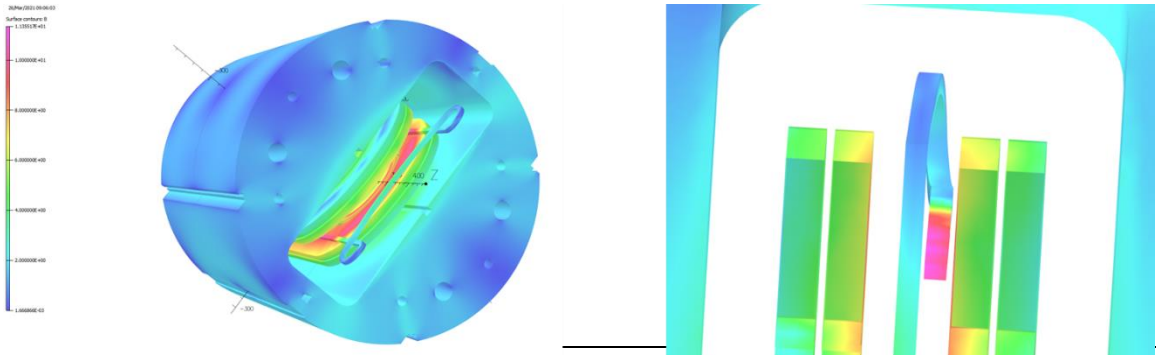

Figure 4.9: Model on the left shows the field contours superimposed over the coils and iron from the end of the magnet and the model on the right shows the cutaway view field contour highlighting highest field (purple) in the straight section region of the insert coil.

Fig. 4.9 shows different views of the field contours from the end of the magnet. Fig. 4.10 shows the results from an OPERA2d model, showing essentially the same features. The maximum computed field at 10 kA is 11.8 T.

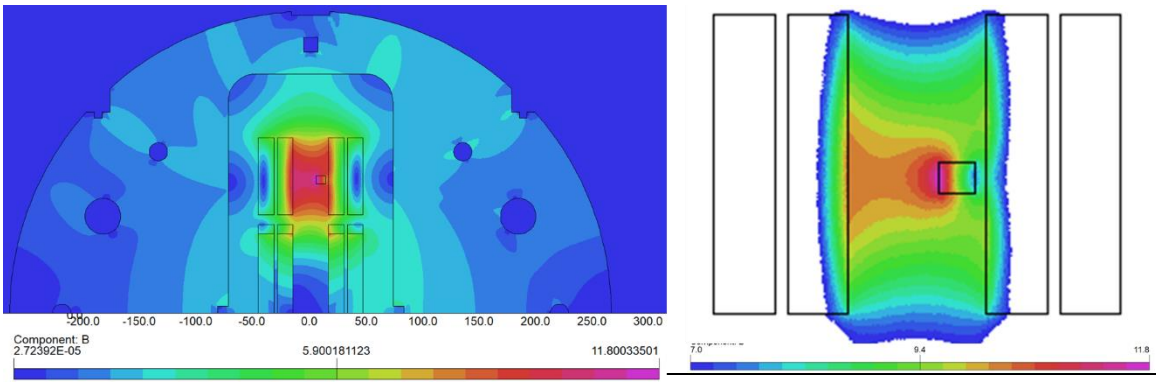

Figure 4.10: 2-d model calculation (generally more accurate than 3-d for the body of the magnet) in the upper-half the of the proof-of-principle demonstration magnet for the overpass/underpass coil.

5.0 Mechanical Design Analysis

The cloverleaf is being designed to allow coil blocks to lift up (or down) to pass over (or under) the beam pipe in such a way as to minimize the strain on the conductor. A detailed mechanical analysis of the overpass/underpass coil and its support system is important for the design of the magnet. We have performed two mechanical analyses: (1) A 3D analysis using COMSOL that models the magnet end region, which includes the clover leaf. The field from the DCC017 coils falls off to about 20% of the field inside the magnet, which reduces the Lorentz forces. The 3D simulations are important for the design of the support structure for the complex end coil. (2) A 2D analysis using ANSYS models a cross section of the DCC017 magnet with the coil in the straight section, where the field is maximum. The coil strain in the straight section will limit the performance of the coil. Both of these analyses depend on the mechanical properties of the materials used. Of particular importance is the modulus of the epoxy impregnated Nb_3Sn coils. We are using the magnet and Nb_3Sn coil material properties documented for the US LARP [21].

5.1 ANSYS Analysis

The straight section of the overpass/underpass coils is in the high field region and subject to large Lorentz forces. The strain in the coil conductor will potentially limit the performance of the coil. A mechanical simulation of the 2D cross section was performed to evaluate the design. Fig. 5.1.1 shows the cross section. The coils are shown in red; a stainless-steel collar that holds the DCC017 coil is shown in purple; magnetic iron for the yoke is shown in cyan; and the open aperture is shown in light blue. Magenta is a pad between the overpass/underpass coil and the DCC017 coil, to spread the local load.

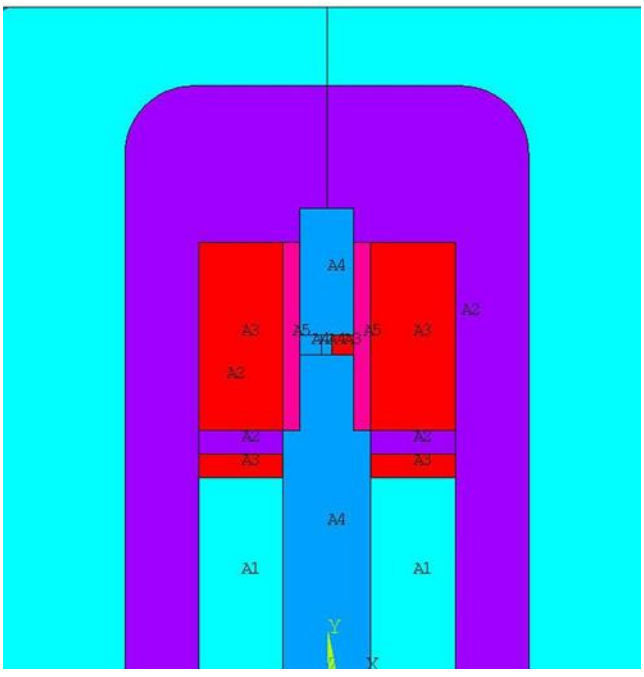

Fig. 5.1.1: Cross section of the overpass/underpass coil in the DCC017 magnet.

Figure 5.1.1 shows the case with a single overpass/underpass coil in the DCC017 magnet. A symmetric case with two overpass/underpass coils was examined but winding two overpass/underpass coils exceeds the Phase II budget.

A magnetic simulation is first performed to predict the field and Lorentz force at each node, to generate input for the structural calculation. Fig. 5.1.2 shows contour plots of the field. On the left is the field inside the iron yoke. On the right is a blowup of the field on the overpass/underpass coil. The peak (median) field on the overpass/underpass coil is 11.7 T (9.6 T), implying a total force on the coil of 480 kN/m.

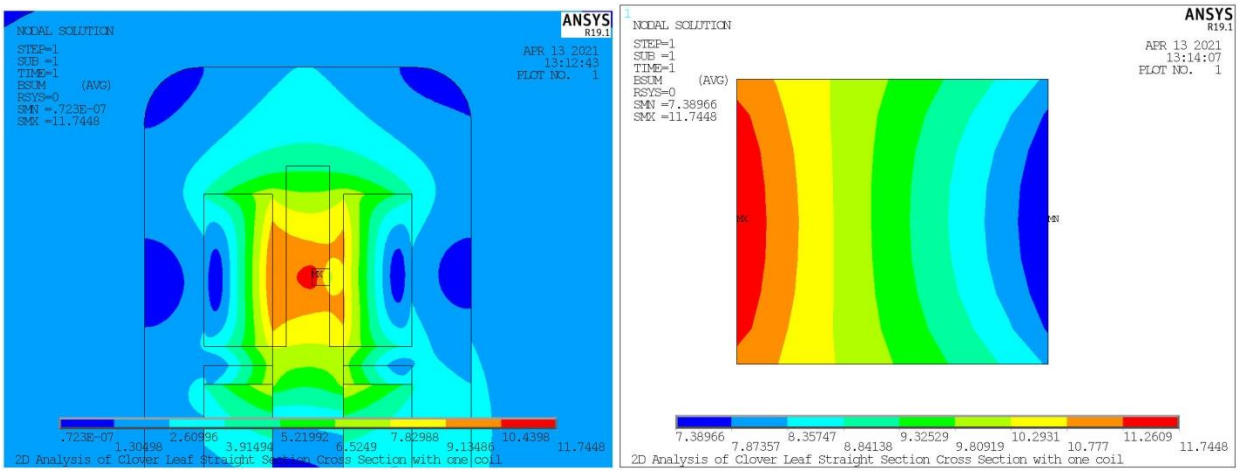

Fig. 5.1.2: Contour plot of |B| over the inside of the yoke (left) and over the overpass/underpass coil (right).

In the second phase of the simulation, stresses and strains are calculated from the Lorentz forces previously saved. Figure 5.1.3 shows a contour plot of the displacement as a result of the forces. The maximum displacement, 128 μm, is in the vicinity of the overpass/underpass coil and the adjacent DCC017 coil. A contour plot of the von Mises stress over the overpass/underpass coil is shown in Fig. 5.1.4. The peak von Mises stress is 217 MPa; the goal was to limit the Nb_3Sn stress to 200 MPa. The peak stress is localized and may be an artifact of the simulation rather than reality. Fig. 5.1.5 shows the von Mises strain at the overpass/underpass coil.

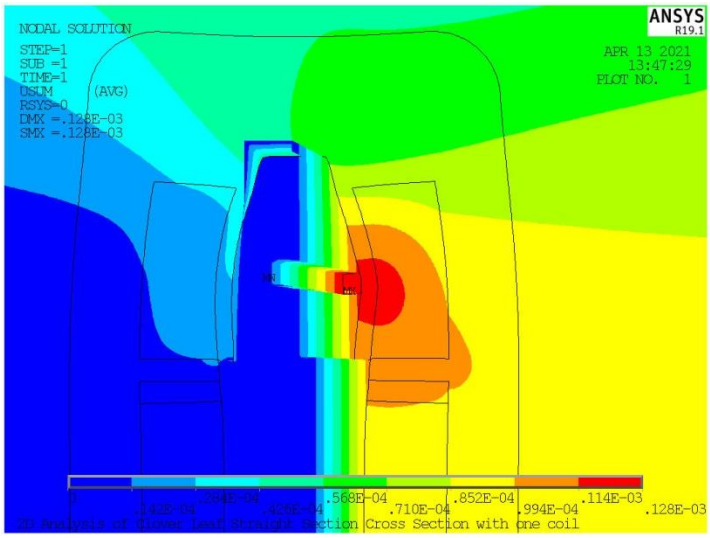

Fig. 5.1.3: Contour plot of the displacements.

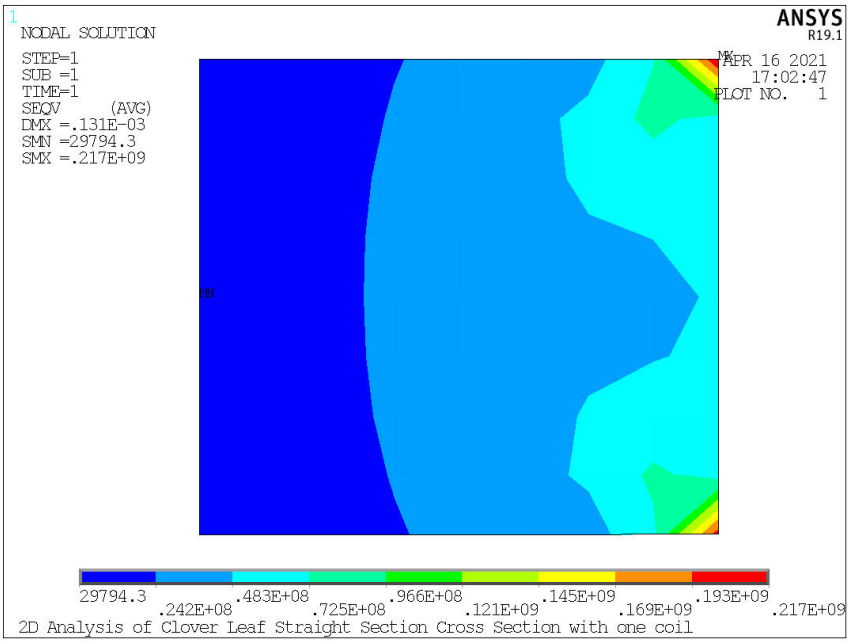

Figure 5.1.4: Contour plot of von Mises stress over the overpass/underpass coil.

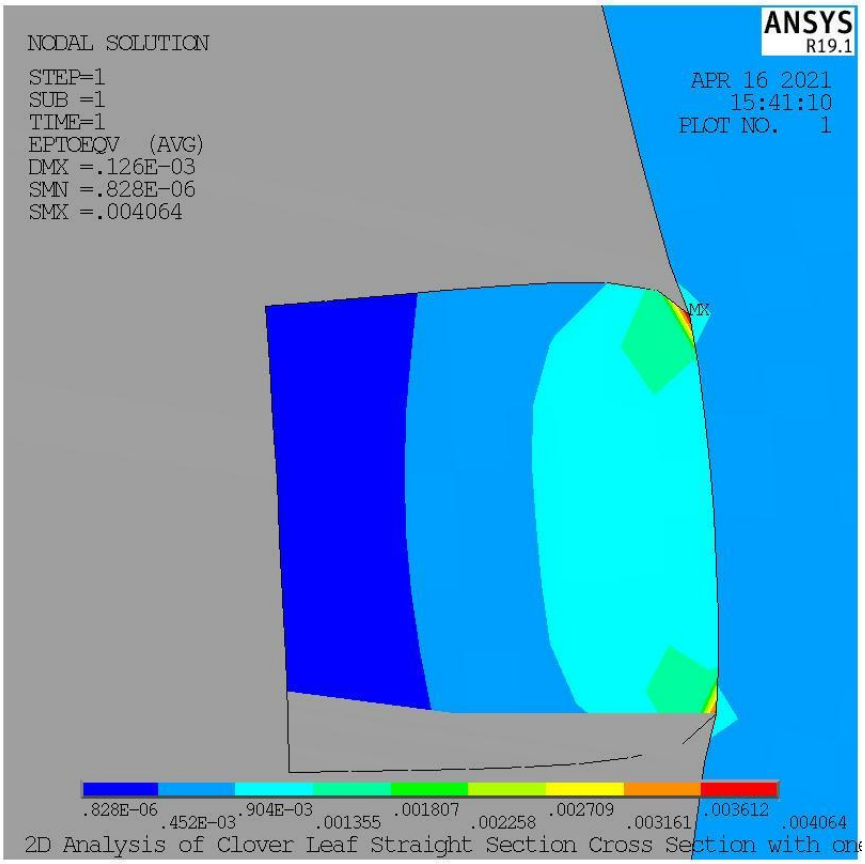

Figure 5.1.5: Contour plot of the von Mises strain.

5.2 3-D Analysis: Field, Displacements, Stresses & Strains in DCC017 & Insert Coil

Excessive strain of Nb_3Sn incurs critical-current degradation, either temporary (reversible) or permanent (irreversible). Therefore, a major goal of the structural analysis described below is to minimize any augmentations of strain in the Nb_3Sn of DCC017. Important also, of course, is that the overpass/underpass coil itself is not at significant risk of conductor degradation.

At its maximum current of 10.8 kA, DCC017 generates a maximum ambient field of 10.6 T. In such an ambient field, a Rutherford cable 1.46 mm thick carrying 10.8 kA experiences a Lorentz bearing pressure of (10.6 T) (10.8 kA) / 1.46 mm = 78 MPa. With a Young's modulus of the cable assumed as 44 GPa, the implied strain is 78 MPa / 44 GPa = 0.18%, an increment that might raise the total strain in the DCC017 Nb_3Sn sufficiently to risk conductor degradation. Therefore, the insert-coil support structure includes a stainless-steel pad, as shown in Fig. 5.2.1, which spreads the Lorentz load from the insert coil onto a much larger surface of DCC017. The pad is 6 mm thick; very gradually, to minimize stress concentrations from abrupt changes in thickness, the pad increases in thickness by another 8 mm at the leg of the overpass/underpass coil, to accommodate a groove for its conductor.

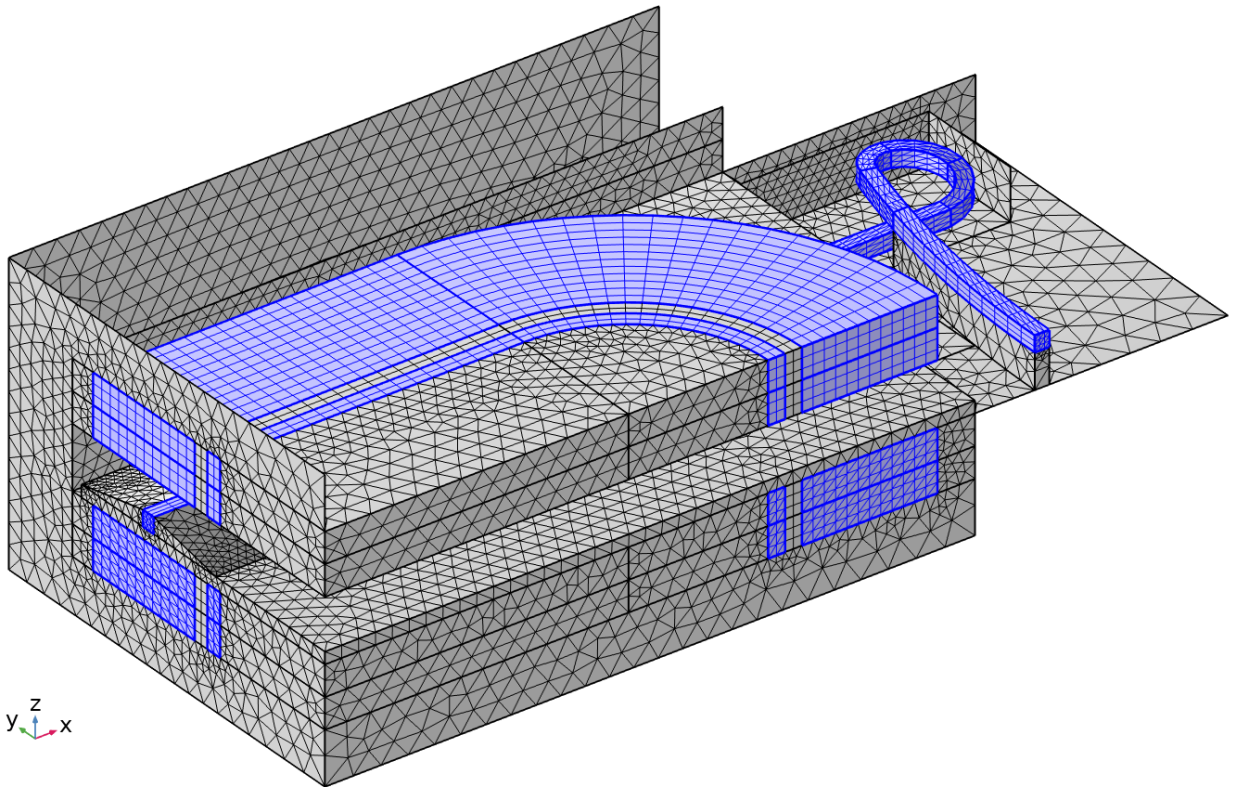

Figure 5.2.1. Mesh (mapped hexahedral and free-tetrahedral) of quadrant of DCC017 coils & collar, five-turn overpass/underpass coil, and stainless-steel support blocks. Many domains and faces are hidden to reveal those of greater interest. Blue is Nb_3Sn.

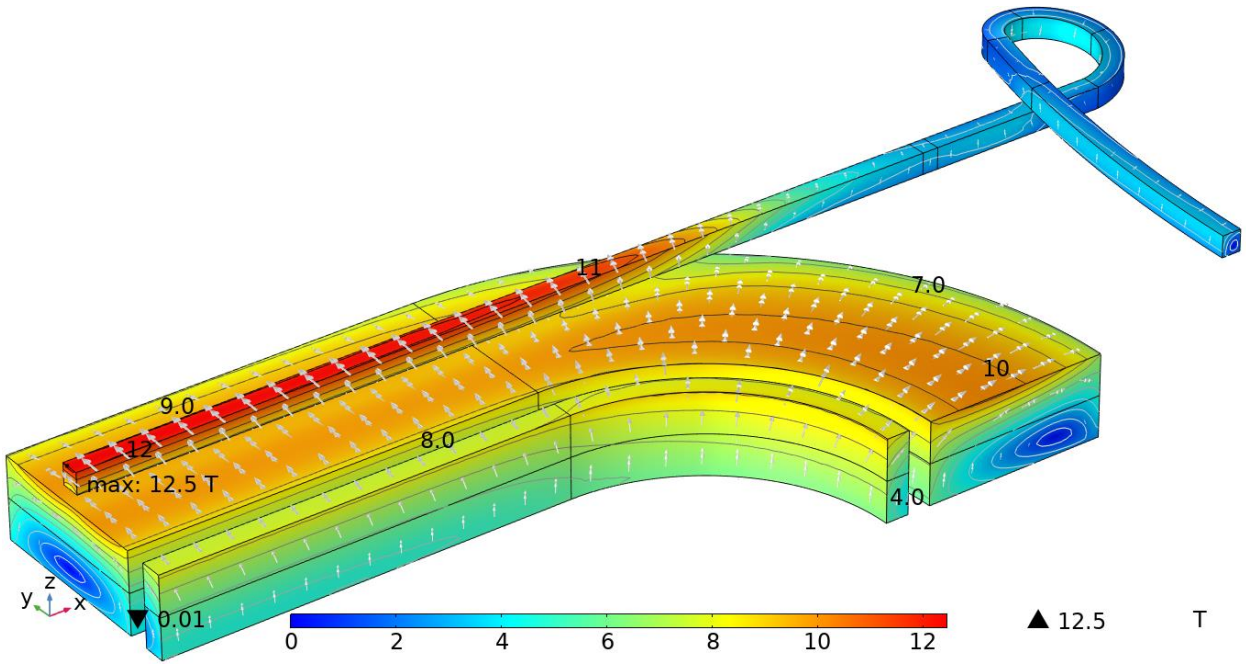

Figure 5.2.2. Magnetic field direction (arrows) and magnitude (color & contours) with 10.8 kA in all coils. Contours are 1 T to 12 T in steps of 1 T.

Lorentz forces on the zones of the overpass/underpass coil are presented in Table IV.

Table IV. Lorentz forces on four zones of the five-turn insert coil at 10.8 kA

overpass-coil zone [leg length = 400 mm]	F_x kN	F_y kN	F_z kN
leg to x_{collar} (326 mm)	0	1.993	-133.3
leg beyond 326 mm	0	0.218	−2.004
Helical ramp [270° − 16°]]	1.760	1.339	0.037
arc R = 510 mm @ 870 mm	4.047	−0.309	-0.881

Figure 5.2.3 predicts the displacements and von Mises stress in DCC017 and the five-turn overpass/underpass coil, with all properties isotropic, and Young's moduli of 200 GPA (stainless steel and magnetic iron), 44 GPa (Nb_3Sn), and 22 GPa (epoxy-fiberglass). The maximum displacement is 0.114 mm, a mere 8% greater than the 0.106 mm with DCC017 operated alone, without the insert coil. In the stainless-steel support structure, the maximum von Mises stress of 194 MPa is 24% greater than the maximum of 157 MPa when operated alone, but the support structure can **reduce** the maximum von Mises stress in the DCC017 Nb_3Sn, from 58 MPa to 44 MPa, if the system can be made to behave monolithically. In the Nb_3Sn of the insert coil, the predicted maximum von Mises stress is 70 MPa.

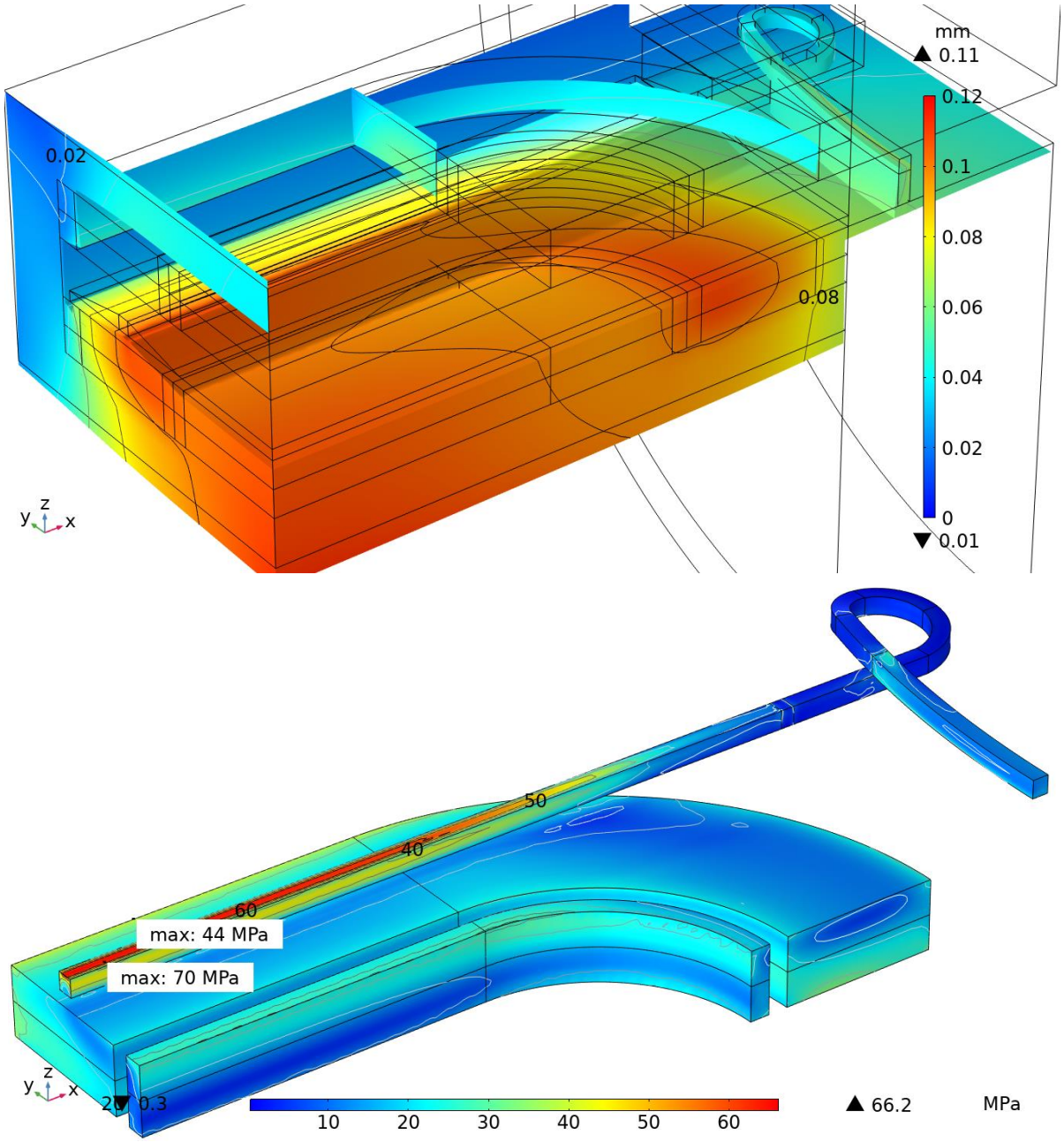

Figure 5.2.3. Top: Displacements, magnified 100-fold; contours are 0.02 mm to 0.10 mm in steps of 0.02 mm. Bottom: von Mises stresses; contours are 10 MPa, 30 MPa and 60 MPa.

Figure 5.2.4 plots the direction and magnitude of the 1st principal stress and strain in the Nb_3Sn of both DCC017 and the overpass/underpass coil, including the magnitudes and locations of the extreme values in each. All values are modest.

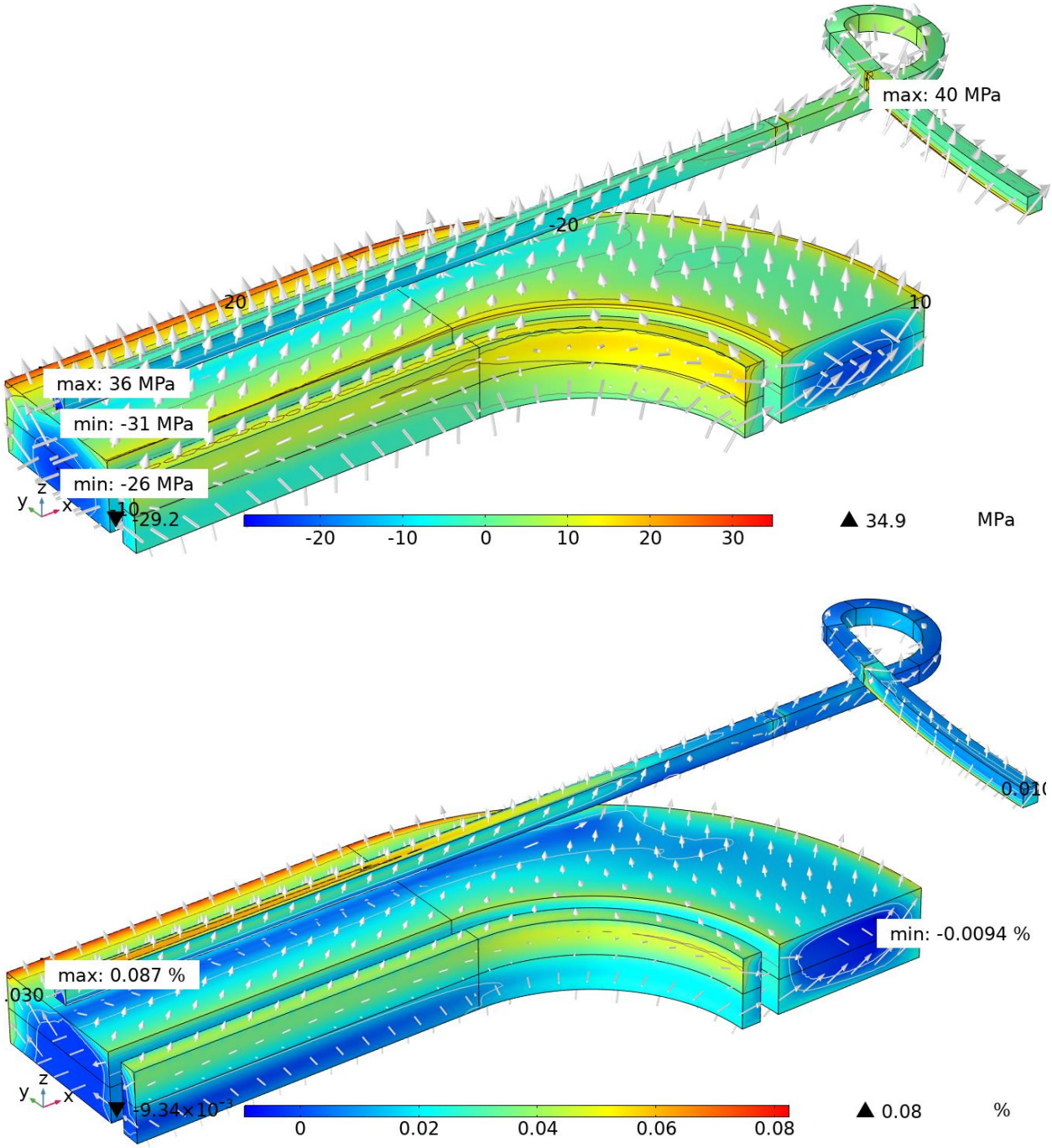

Figure 5.2.4a&b. 1st principal stress and strain in Nb_3Sn. Top: 1st principal stress; MPa contours are −20 to 20 in steps of 10. Bottom: 1st principal strain; contours are [0, 0.01%, 0.03%, 0.06%].

Figure 5.2.5 plots the direction and magnitude of the 2nd principal stress and strain in the Nb_3Sn of both DCC017 and the overpass/underpass coil, including the magnitudes and locations of the extreme values in each. The stresses and strains are small everywhere.

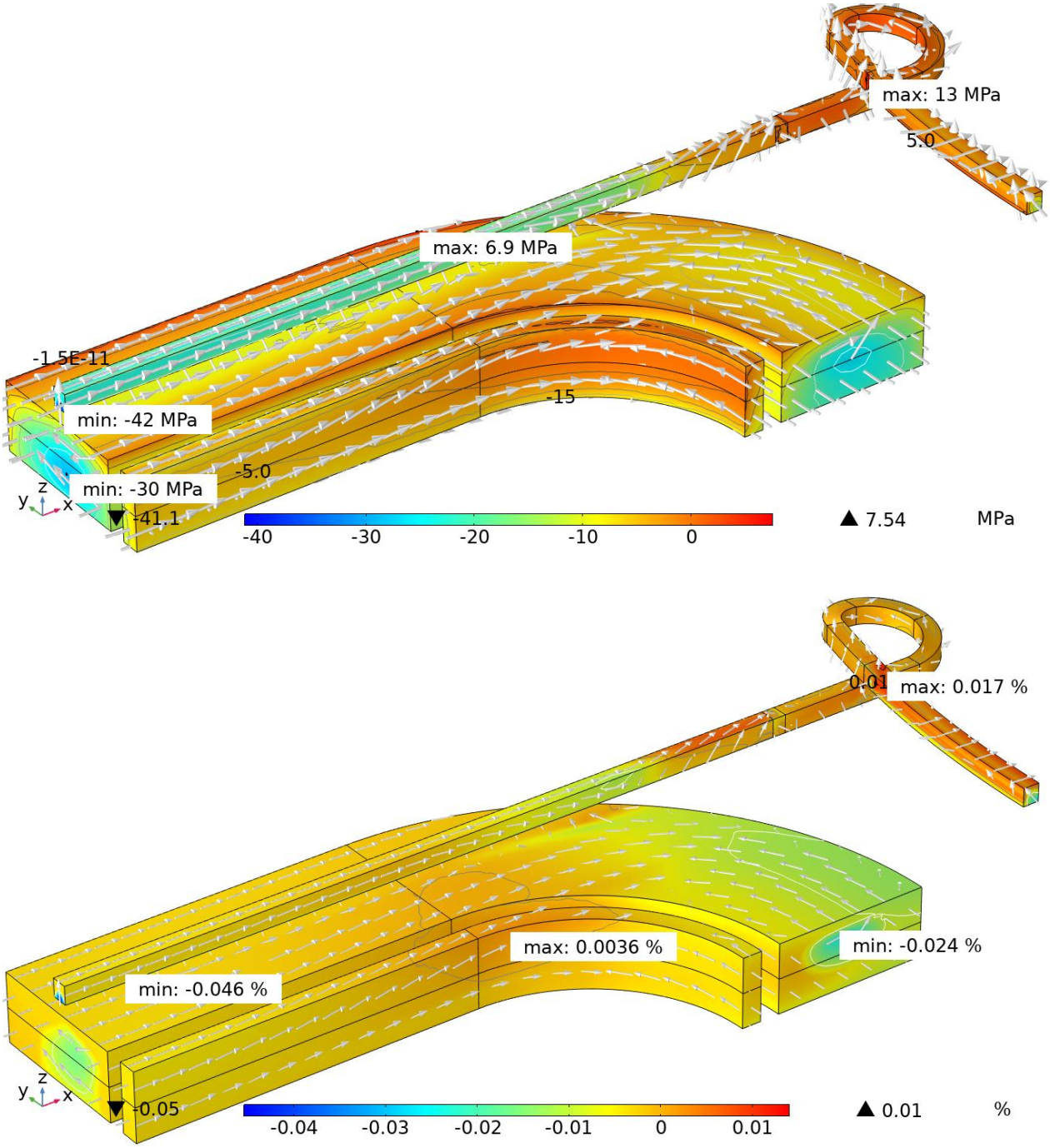

Figure 5.2.5a&b. 2nd principal stress and strain in Nb_3Sn. Top: 2nd principal stress; MPa contours are −25 to 5 in steps of 5. Bottom: 2nd principal strain; contours are [−0.01%, 0, and 0.01%.

Figure 5.2.6 plots the direction and magnitude of the 3rd principal stress and strain in the Nb_3Sn of both DCC017 and the overpass/underpass coil, including the magnitudes and locations of the extreme values in each. The bearing pad under the insert-coil leg spreads the load well, limiting the strain to 0.10% in DCC017 and 0.016% in the overpass/underpass coil.

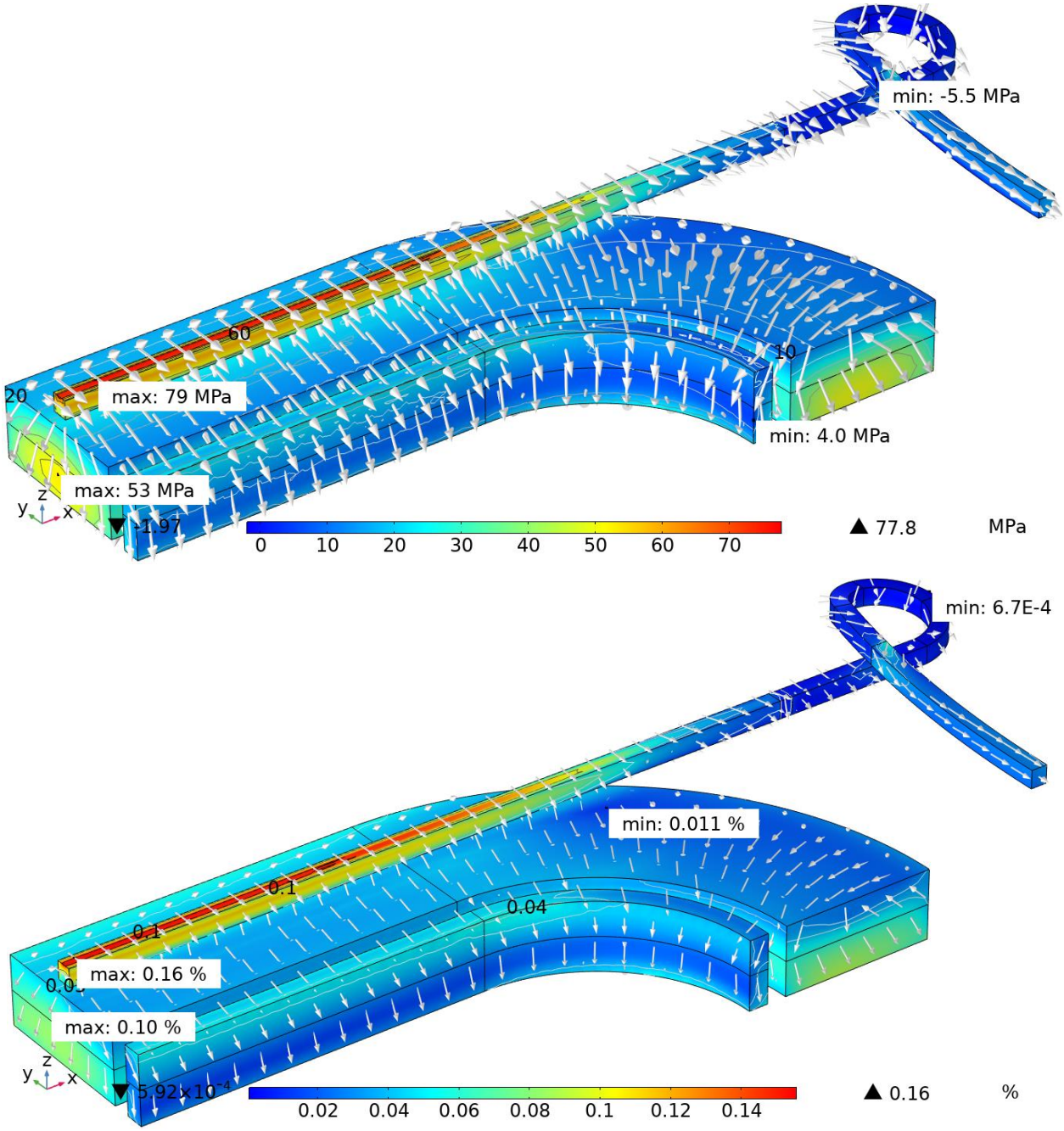

Figure 5.2.6a&b. Negative 3rd principal stress and strain in Nb_3Sn. Top: Negative 3rd principal stress; MPa contours are 0 to 70 by 10. Bottom: Negative 3rd principal strain; contours are [0.01%, 0.03%, 0.06%, 0.10%, 0.15%].

6.0 Preliminary Engineering Design of Proof-of-Principle Coil for Phase II

The preliminary mechanical engineering design for the fabrication and installation of a Nb_3Sn "Overpass/Underpass" ("OP/UP") coil in the aperture of the existing Common Coil DCC017 magnet was completed. The single coil design followed the magnetic model in terms of the placement of the coil blocks at the two poles of the main coils to provide the greatest field. The ends of the coil were located beyond the central field of the magnet to reduce the magnetic forces in the end regions. The transverse ends between the "cloverleafs" of the coil were designed with a convex curve, as the CERN OP/UP coil, to facilitate conductor contact with the winding surface in these regions.

The design is based on a continuous winding form to ensure the proper dimensions and shape of the completed coil. This form, as is seen in Figure 6.1, becomes a permanent part of the coil support structure; as such, it needs to be compatible with all the fabrication steps involved.

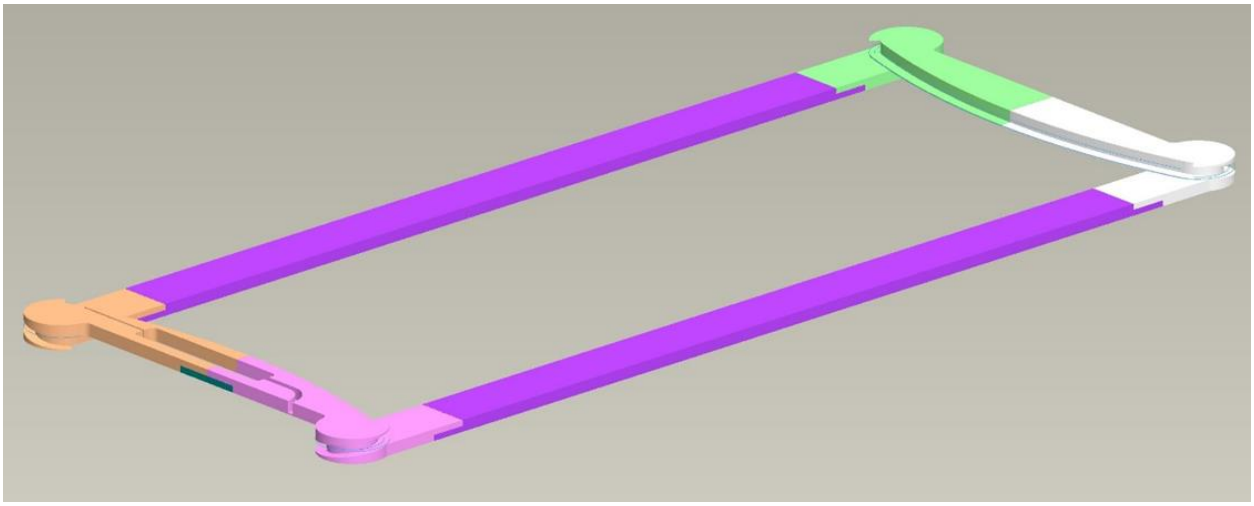

Figure 6.1: Coil winding form.

In particular, as the niobium tin coil is being fabricated using the wind-and-react process, the coil form must be compatible with the 665 C reaction temperature. Therefore, all components are designed to be made from titanium, including the 3-D end shapes, which will be fabricated using additive machining, and which survives the heat exposure and is well matched to the thermal expansion of the conductor during reaction. Nonetheless, gaps are still required between mating titanium frame components as is seen in Figure 6.2.

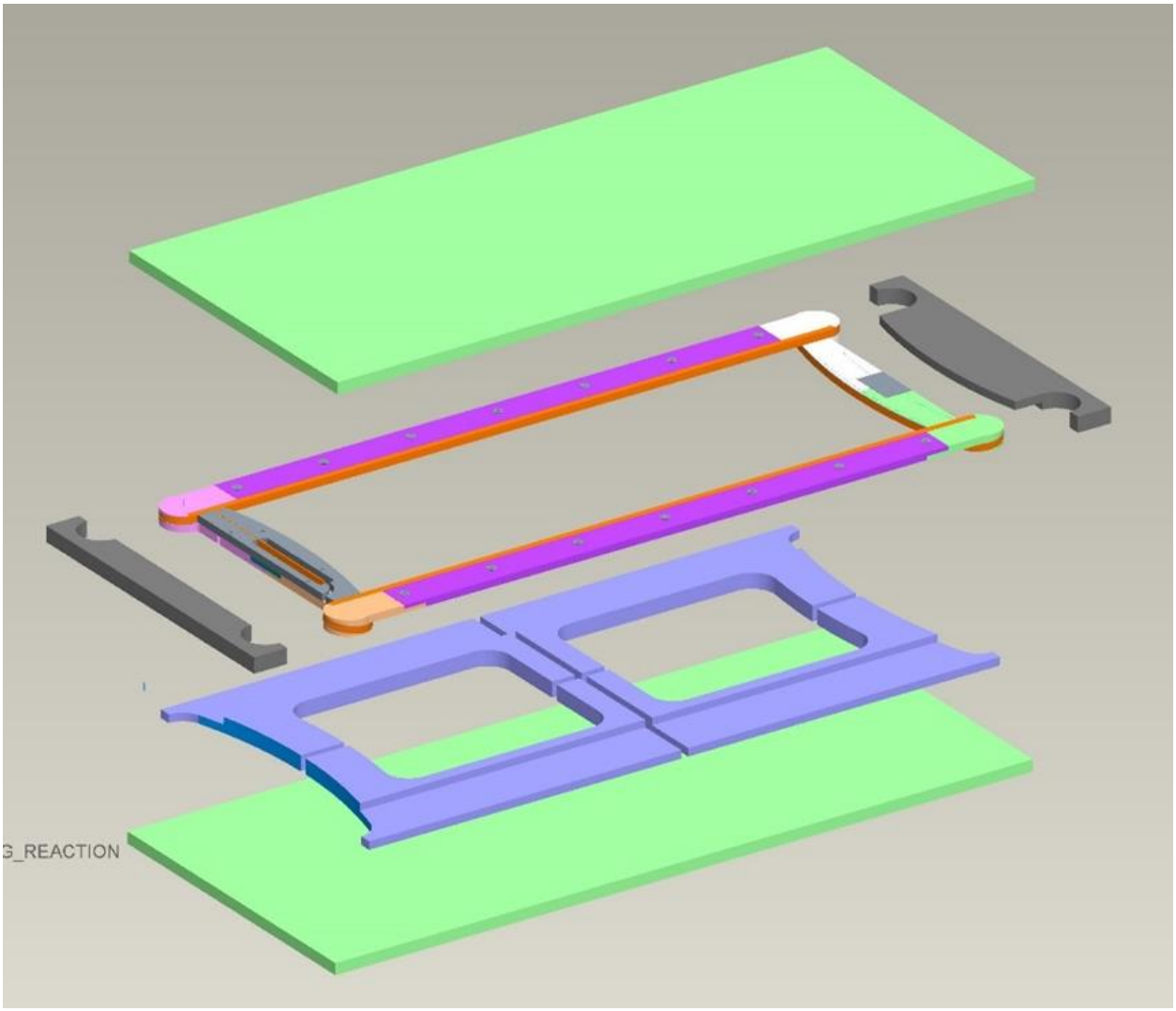

Figure 6.2: Exploded view of tooling showing gaps in (blue) reaction frames.

The winding form does include some temporary components, namely lateral guide plates, which are subsequently removed. After winding, additional clamping is introduced to the exposed edges of the wound coil to ensure proper dimensioning and positioning of the coil block during reaction, and the coil is installed in an oven and heated using a prescribed cycle to a plateau of 210C for 48 hours, then 395C for 48 hours, and then finally 665C for 50 hours for the reaction to be completed. The coil is then cooled using a similar prescription. It may be mentioned that the gaps will also be present in the straight sections and convex sections of the ends to allow for the differential thermal expansion between various metals and the conductor during reaction.

After reaction, cleaning and testing are performed, after which instrumentation and niobium titanium exiting leads are spliced within the coil structure as seen in Figure 6.3.

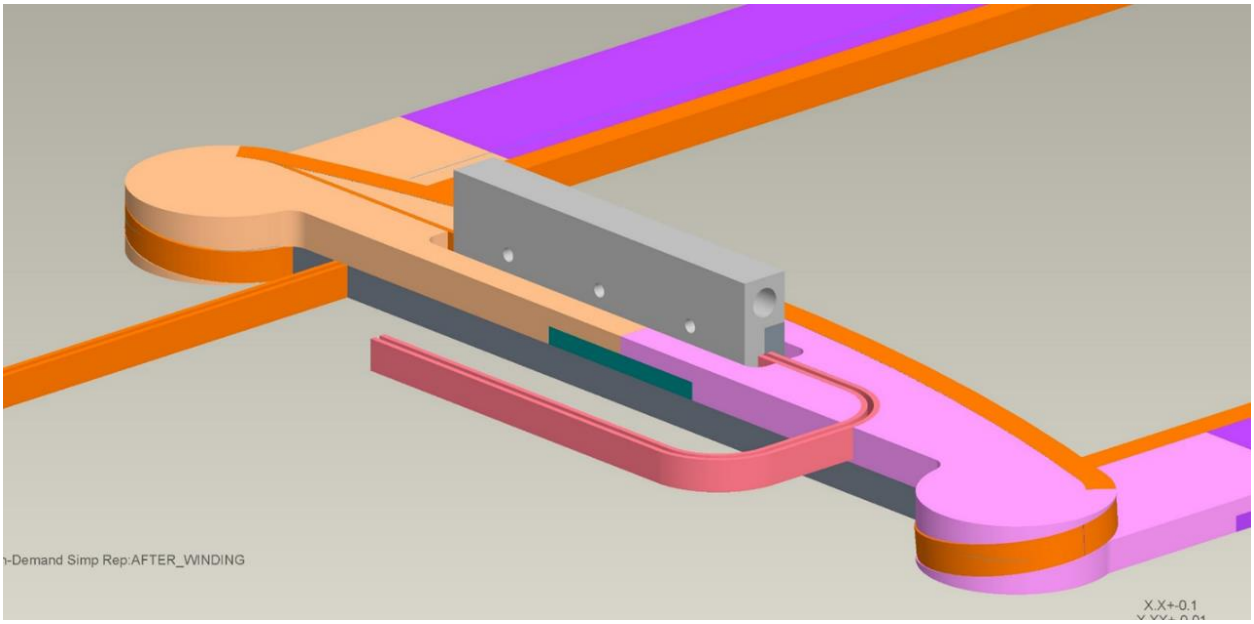

Figure 6.3. Nb_3Sn coil lead to NbTi exiting lead splice within the impregnated coil structure.

In this way, after impregnation the brittle niobium tin conductor is protected within the impregnated coil volume, and only ductile niobium titanium and copper conductors exit the coil structure. Additional final coil components are added as shown in Figure 6.4, and then the coil is vacuum pressure impregnated using CTI-101K epoxy at elevated temperature.

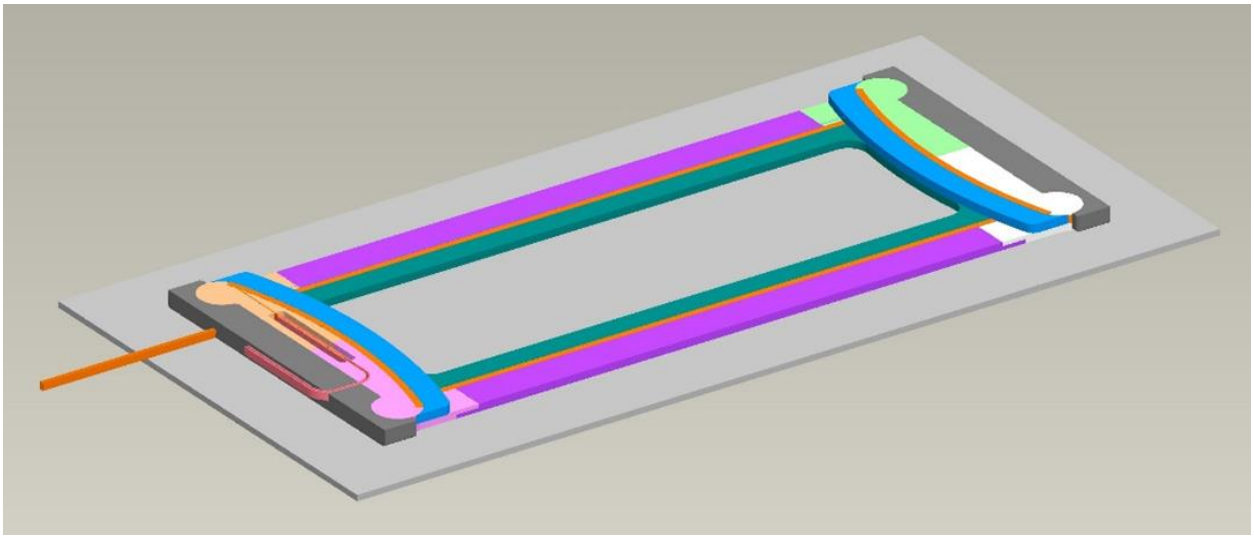

Figure 6.4. Nb_3Sn coil in the impregnation fixture.

After impregnation, final structure plates are added to connect and support coil blocks together, and at installation additional load distribution plates are added between the coil and the DCC017 main coils to reduce contact stress experienced by the main coils.

Considerable effort was made to ensure that the design was compatible with the plan to install two similar coils as a pair into DCC017, if future funding permits. This involved strategically shifting the ends of the coils in the axial direction to enable the coil ends to be nested laterally, thereby having the two coils occupy only 50% greater space than one coil, as shown in Figures 6.5 and 6.6. Additionally, changes to the design of the single coil lead were required to be able to connect the two coils in series if needed.

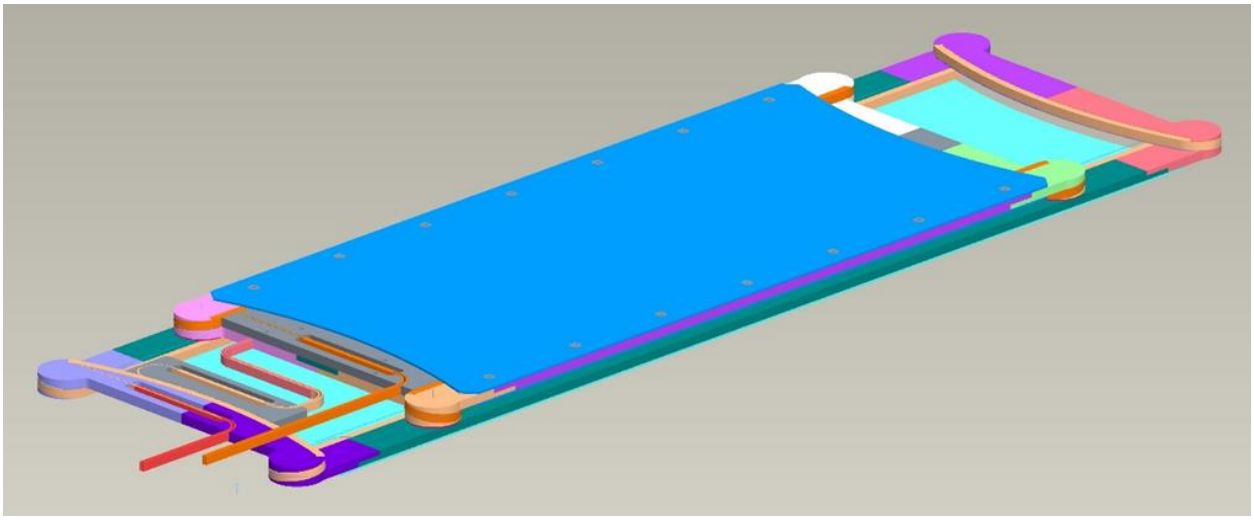

Figure 6.5. Two OP/UP coils with staggered ends nested together.

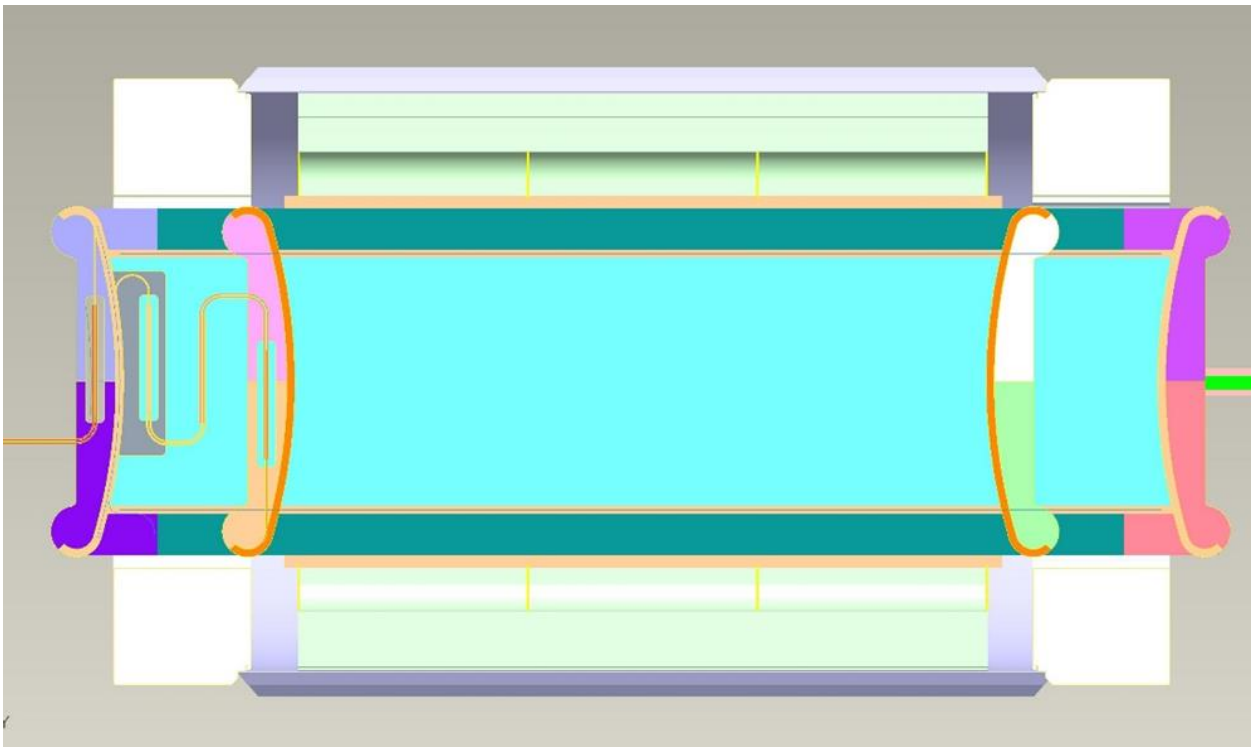

Figure 6.6. Section view of two OP/UP coils in DCC017.

Figure. 6.7 shows the 3-d rendering of the overpass/underpass coils inside the magnet DCC017.

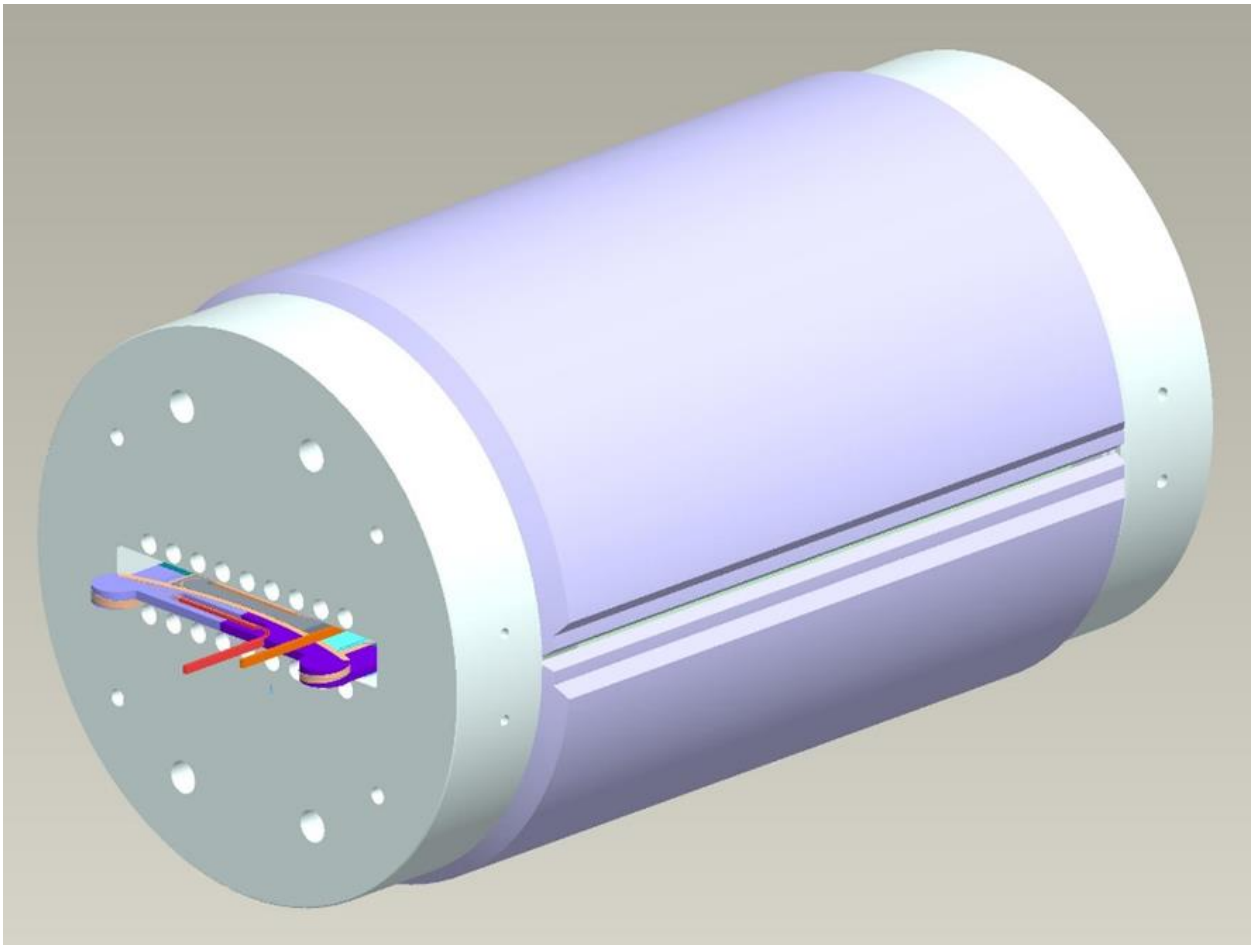

Figure 6.7. Design view of the OP/UP coils assembled in the magnet DCC017.

7.0 Construction of Parts and Winding of the Overpass/Underpass Coil

An important part of the Phase I plan was to do a practice winding of the coil having a new shape. Use of the 3-d printer purchased during an earlier PBL SBIR, allowed a series of relatively complex parts to made and iterated. Fig. 7.1 shows the different views of overpass/underpass printed parts and one turn wound, including the initial practice run of how the cable will lay in the overpass/underpass section. Fig. 7.1 (left) shows the 3-d printed parts for the overpass/underpass section, Fig. 7.1 (middle) shows an initial study of how the cable is going to lay in the overpass/underpass section, and Fig. 7.1 (right) shows the first turn of the lower dipole coil based on the overpass/underpass geometry. The arrow shows the beam path and an illustration of how the overpass/underpass block coil geometry clears the beam tube.

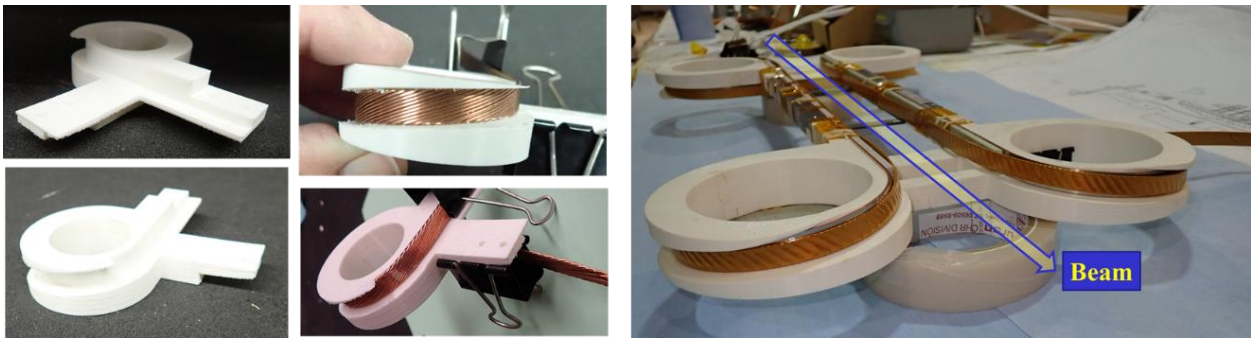

Figure 7.1. Left: 3-d printed parts for the overpass/underpass section, Middle: initial study of how the cable is going to lay in the overpass/underpass section, and Right: first turn of the lower dipole coil based on the overpass/underpass geometry. The arrow shows the beam path and an illustration of how overpass/underpass block coil geometry clears the beam tube.

We performed two distinct styles of practice windings. As mentioned earlier, CERN is also pursuing the overpass/underpass design (also named the cloverleaf design) for their 20 T dipole design [14]. Both projects are benefitting from ongoing discussions and collaboration. A specific feedback from the CERN team is described here. Fig. 7.2 (left) shows the 1-turn coil wound as per the original design and Fig. 7.2 (right) shows the HTS tape wound at CERN as per the modified geometry developed there. The convex shape between the two cloverleaves or underpass/overpass sections allows the cable to lay nicely. Therefore, that general shape was adapted during the remaining part of Phase I and also in our Phase II proposal. In both cases, 3-d printer technology was used to save cost and time.

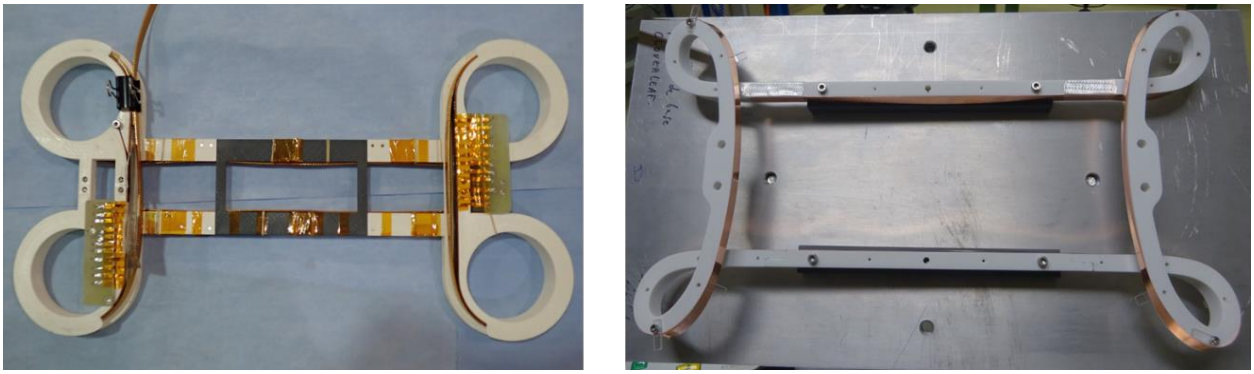

Figure 7.2. Left: Rutherford cable coil wound by the PBL/BNL team in the earlier part of the Phase I proposal with a straight connect between the two overpass/underpass (cloverleaf) sections in the end. Right: HTS tape coil wound by the CERN team with a convex connect between the two cloverleaf (overpass/underpass) sections in the end.

Fig. 7.3 shows the assembly of the printed curved parts (black) and machined straight parts made with Aluminum (gray) to make a frame for winding the overpass/underpass practice coil with a convex connect between the cloverleaf sections. The two pictures on the left and right side are the views of the same frame turned over to show the other side.

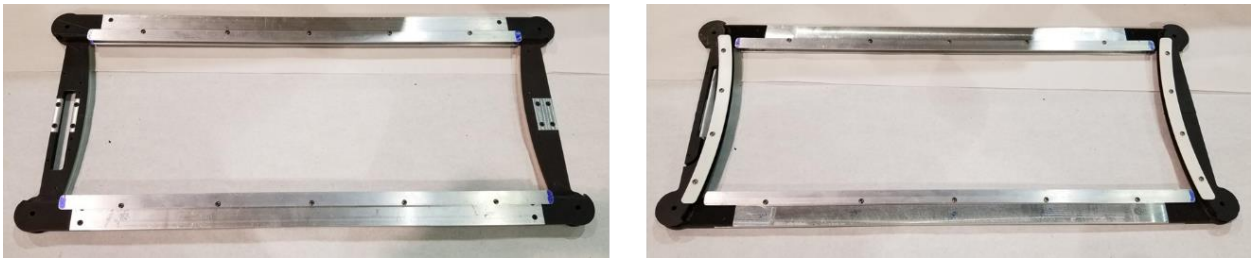

Figure 7.3. Frame for winding the overpass/underpass coil assembled with the printed curved parts (black) and machined straight Aluminum parts (gray). Two pictures on the left and right side are the views of the same frame turned over to show the other side.

Fig. 7.4 shows the winding of the Phase I overpass/underpass practice coil with the Rutherford cable. It is similar to the Nb_3Sn Rutherford cable that will be used in winding the actual coil in Phase II. The two pictures on the left and right side are views of the same coil turned over to show the other side.

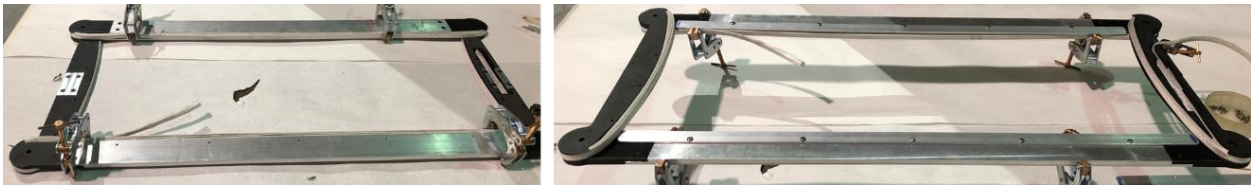

Figure 7.4. Phase I winding of the overpass/underpass coil with a similar Nb_3Sn Rutherford cable that will be used in winding the Phase II coil. Two pictures on the left and right side are views of the same coil turned over to show the other side.

Fig. 7.5 and Fig. 7.6 show different views of the same overpass/underpass Phase I coil wound with Nb_3Sn Rutherford cable.

Figure 7.5. Views of the Phase I overpass/underpass coil from different angles.

Figure 7.6. More views of the Phase I overpass/underpass coil from different angles.

Fig. 7.7 shows a view of the mockup insertion test of this coil is shown inside the common coil dipole DCC017. Phase II coil will be enclosed in a support structure before it is inserted inside.

Figure 7.7. A view of the mockup insertion test of the overpass/underpass coil in DCC017.

8.0 Summary

The goal of this project is to develop an innovative overpass/underpass (also called cloverleaf) coil design for the ends of high field block coil dipoles. To avoid excessive strain, particularly for brittle conductor such as Nb_3Sn or HTS, the cable in certain blocks must be lifted or bent in the hard direction gradually to clear the beam tube making the ends excessively long and prone to degradation. The overpass/underpass geometry replaces the hard bend by a gentle twist and significantly reduces the length. The end geometry is, however, new, and more complex.

The purpose of the upcoming Phase II proposal is to develop and demonstrate the overpass/underpass for a proof-of-principle Nb_3Sn dipole with a field exceeding 10 T. The primary purpose of Phase I was to develop and perform a magnetic and mechanical analysis for that proof-of-principle dipole, wind a practice coil and to complete a conceptual design.

We exceeded the original goals of Phase I by developing a preliminary engineering design (rather than just a conceptual design) with significant details. The project also benefitted from collaboration with a CERN team which is also pursuing an overpass/underpass design for their 20 T dipole design with Roebel cable. We wound two practice coils rather than one using the printed part technology. The original design with straight connections was replaced by a CERN-style convex connection between two overpass/underpass (or cloverleaf) sections and the new design is adopted for Phase II.

Significant magnetic and mechanical design and analysis work has also been performed for the proof-of-principle 11 T dipole. 16 T design work will be carried out in Phase II.

We were also able to locate Nb3Sn cable (leftover from previous projects), often a long lead time item. This is a proven cable and is well suited for Phase II.

This report summarizes the considerable work progress made during Phase I which puts us in a good position to make a strong Phase II proposal to achieve a positive outcome of this project via a proof-of-principle ~11 T Nb_3Sn dipole demonstration. The work will also be presented at the 27^{th} International Conference on Magnet Technology (MT27) for which an abstract has already been submitted [22]. Once the design is successfully demonstrated, the overpass/underpass end geometry is likely to be used in other block coil designs beyond just the common coil.

9.0 References

1. The Particle Physics Project Prioritization Panel (P5) and its subpanel on Accelerator R&D, http://science.energy.gov/hep/hepap/.
2. R. Gupta, *et al.*, "Next Generation IR Magnets for Hadron Colliders," Presented at the Applied Superconductivity Conference at Houston, TX, USA (2002).
3. A. Koski and S.L. Wipf, "Computational Design Study for an Accelerator Dipole in the range of 15-20 T," *IEEE Transactions on Magnetics, Vol. 32, No. 4, July 1996.*
4. W. Sampson, unpublished (1980).
5. P. Ferracin, et al., "Recent Test Results of the High Field Nb_3Sn Dipole Magnet HD2," *IEEE Transactions on Applied Superconductivity*, Vol. 20, No. 3, June 2010.
6. A. Milanese, et al., "Design of the EuCARD High Field Model Dipole Magnet FRESCA2," *IEEE Transactions on Applied Superconductivity*, Vol. 22, No. 3, June 2012.
7. A. McInturff, et al., "Current Status of the Texas A&M Magnet R&D Program," *IEEE Transactions on Applied Superconductivity*, Vol. 21, No. 3, June 2011.
8. R.C. Gupta, "A Common Coil Design for High Field 2-in-1 Accelerator Magnets," 1997 Particle Accelerator Conference in Vancouver, Canada (1997).
9. M. Takayasu, L. Chiesa, P.D. Noyes, and J.V. Minervini, "Investigation of HTS Twisted Stacked-Tape Cable (TSTC) Conductor for High-Field, High-Current Fusion Magnets," *IEEE Transactions on Applied Superconductivity*, Vol. 27, No. 4, June 2017.
10. J. van Nugteren, G. Kirby, J. Murtomaki, G. de Rijk, L. Rossi and A. Stenvall, "Towards REBCO 20+ T Dipoles for Accelerators," presented at the European Conference on Applied Superconductivity (EUCAS 2017), September 2017.
11. J. van Nugteren, "High Temperature Superconductor Accelerator Magnet", Page 46-47, https://cds.cern.ch/record/2228249/files/CERN-THESIS-2016-142.pdf .
12. J. van Nugteren, J. Murtomäki, G. Kirby, T. Nes, G. de Rijk, L. Bottura and L. Rossi, "Design and Optimization of a Full HTS Accelerator Dipole for Achieving Magnetic Fields Beyond 20 T," poster presented at the 2018 Applied Superconductivity Conference, Seattle, USA.
13. J. S. Murtomäki, J. van Nugteren, A. Stenvall, G. Kirby and L. Rossi, "3-D Mechanical Modeling of 20 T HTS Clover Leaf End Coils—Good Practices and Lessons Learned," in *IEEE Transactions on Applied Superconductivity*, vol. 29, no. 5, pp. 1-8, Aug. 2019, Art no. 4004608, doi: 10.1109/TASC.2019.2899317.
14. https://www.researchgate.net/project/Dipole-HTS-Magnets-at-CERN
15. R. Gupta, C. Rey, et al., Presentation and Posters at 2016 Low Temperature Superconductor Workshop," Santa Fe, NM, February 8-10, 2016; one presentation available at https://www.bnl.gov/magnets/staff/gupta/Talks/ltsw16/gupta-ltsw16-poster.pdf https://www.bnl.gov/magnets/Staff/Gupta/Talks/ltsw16/gupta-ltsw16-presentation.pdf.
16. R. Gupta, et al., "React & Wind Nb_3Sn Common Coil Dipole," 2006 Applied Superconductivity Conference, Seattle, WA, USA, August 27-September 1, 2006.
17. R. Gupta, et al., "Design, Construction and Test of HTS/LTS Hybrid Dipole," International Conference on Magnet Technology (MT-25), Amsterdam (2017).
18. R. Gupta et al., "New Approach and Test Facility for High-Field Accelerator Magnets R&D," in *IEEE Transactions on Applied Superconductivity*, vol. 30, no. 4, pp. 1-6, June 2020, Art no. 4000106, doi: 10.1109/TASC.2019.2961064.
19. J. Muratore, et al, "Test Results of LARP 3.6 m Nb_3Sn Racetrack Coils Supported by Full-Length and Segmented Shell Structures, *IEEE Transactions on Applied Superconductivity*, 19 (2009) 3, 1212-1216, DOI 10.1109/TASC.2009.2018511, June 5, 2009].

20. R. Gupta, et al., Common Coil Dipoles for Future High Energy Colliders, 2016 Applied Superconductivity Conference, Denver, September 4-9, 2016 .
21. H. Felice et al., “Magnetic and Mechanical Analysis of the HQ Model Quadrupole Designs for LARP,” in *IEEE Transactions on Applied Superconductivity*, vol. 18, no. 2, pp. 281-284, June 2008, doi: 10.1109/TASC.2008.921941.
22. R. Gupta, M. Anerella, J. Avronsart, J. Cozzolino, P. Joshi, P. Kovach, and J. Schmalzle, S. Kahn, J. Kolonko, D. Larson, R. Scanlan, R. Weggel, E. Willen and A. Zeller, “Proof-of-Principle Demonstration of a Novel Overpass/Underpass High Field Dipole (Abstract)”, MT27 - International Conference on Magnet Technology, to be held at Fukuoka International Congress Center, Fukuoka, Japan from November 15 to 19, 2021.